Rac1 is deactivated at integrin activation sites through an IQGAP1–filamin-A–RacGAP1 pathway

Guillaume Jacquemet[1], Mark R. Morgan[1], Adam Byron[2], Jonathan D. Humphries[1], Colin K. Choi[3], Christopher S. Chen[3], Patrick T. Caswell[1] and Martin J. Humphries[1,*]

[1]Wellcome Trust Centre for Cell-Matrix Research, Faculty of Life Sciences, University of Manchester, Manchester M13 9PT, UK
[2]Edinburgh Cancer Research UK Centre, Institute of Genetics and Molecular Medicine, University of Edinburgh, Edinburgh EH4 2XR, UK
[3]Department of Bioengineering, University of Pennsylvania, Philadelphia, PA 19104, USA

*Author for correspondence (martin.humphries@manchester.ac.uk)

Accepted 12 June 2013
Journal of Cell Science 126, 4121–4135

doi: 10.1242/jcs.121988

Summary

Cell migration makes a fundamental contribution to both normal physiology and disease pathogenesis. Integrin engagement with extracellular ligands spatially controls, via the cyclical activation and deactivation of the small GTPase Rac1, the dynamic membrane protrusion and cytoskeletal reorganization events that are required for directional migration. Although the pathways that control integrin-mediated Rac1 activation are reasonably well defined, the mechanisms that are responsible for switching off activity are poorly understood. Here, proteomic analysis of activated integrin-associated complexes suggests filamin-A and IQ-motif-containing GTPase-activating protein 1 (IQGAP1) as candidates that link β1 integrin to Rac1. siRNA-mediated knockdown of either filamin-A or IQGAP1 induced high, dysregulated Rac1 activity during cell spreading on fibronectin. Using immunoprecipitation and immunocytochemistry, filamin-A and IQGAP1 were shown to be part of a complex that is recruited to active β1 integrin. Mass spectrometric analysis of individual filamin-A, IQGAP1 and Rac1 pull-downs and biochemical analysis, identified RacGAP1 as a novel IQGAP1 binding partner. Further immunoprecipitation and immunocytochemistry analyses demonstrated that RacGAP1 is recruited to IQGAP1 and active β1 integrin, and that suppression of RacGAP1 expression triggered elevated Rac1 activity during spreading on fibronectin. Consistent with these findings, reduced expression of filamin-A, IQGAP1 or RacGAP1 triggered unconstrained membrane protrusion and disrupted directional cell migration on fibrillar extracellular matrices. These findings suggest a model whereby integrin engagement, followed by filamin-A, IQGAP1 and RacGAP1 recruitment, deactivates Rac1 to constrain its activity spatially and thereby coordinate directional cell migration.

Key words: FLNa, IQGAP1, Integrin, Migration, Rac1, RacGAP1

Introduction

Cell migration is a fundamental physiological process required for embryogenesis, immune surveillance and wound healing. Migration is also central to the regulation of disease pathogenesis by contributing to processes such as tumour invasion and leukocyte transmigration. Integrin receptors provide a physical link between the extracellular matrix (ECM) and the actin cytoskeleton, and serve as platforms for the assembly of signalling complexes that control cell phenotype, including migration (Hynes, 2002). Integrin function is regulated by a conformational switch that modulates extracellular ligand-binding affinity. Inactive integrins exist in a bent conformation and have a low affinity for their ligands, whereas primed or activated integrins are extended and have a high affinity for their ligands (Askari et al., 2009). Integrin-mediated adhesion modulates the activity of the small GTPase Rac1 (Del Pozo and Schwartz, 2007; Morgan et al., 2007; Price et al., 1998), and therefore dynamically regulates cell migration by promoting cytoskeletal re-organisation and membrane protrusion (Ridley, 2003; Ridley, 2006). Disruption of Rac1 signalling results in major migration defects, such as loss of cell directionality on fibrillar matrices (Bass et al., 2007; Pankov et al., 2005) and suppressed wound healing *in vivo* (Liu et al., 2009; Tscharntke et al., 2007). Productive cell migration requires coordinated activation and deactivation of Rac1, and accordingly a range of guanine nucleotide exchange factors (GEFs) and GTPase activating proteins (GAPs) have been reported to be involved in integrin-dependent Rac1 regulation (Katoh and Negishi, 2003; Nishiya et al., 2005). However, the mechanism whereby integrin activation coordinates Rac1 activity is still only partially resolved.

In this study, which builds on published proteomic analyses of fibronectin (FN)-induced, integrin-associated complexes (Humphries et al., 2009; Kuo et al., 2011; Schiller et al., 2011), network analyses were used to identify filamin-A (FLNa) and IQ-motif-containing GTPase activating protein 1 (IQGAP1) as putative links between β1 integrin and Rac1. The hypothesis that FLNa and IQGAP1 modulate integrin-dependent Rac1 activation was tested and the mechanism elucidated. Specifically, FLNa and IQGAP1 are recruited to active integrins to constrain Rac1 activity via the recruitment of the GTPase-activating protein RacGAP1 (also known as MgcRacGAP and CYK4) in order to restrict protrusive activity during cell migration. These findings reveal a novel function for a FLNa–IQGAP1 complex in the regulation of Rac1 activity upon integrin activation.

Results

FLNa and IQGAP1 suppress Rac1 activity downstream of FN–integrin engagement

To identify new mechanisms by which β1 integrin regulates Rac1 activity, data from three proteomic analyses of FN-induced,

integrin-associated complexes (Humphries et al., 2009; Kuo et al., 2011; Schiller et al., 2011) were integrated with protein–protein interaction (PPI) databases, to generate a hypothetical FN-induced, integrin-associated PPI network. Analysis of the components connecting β1 integrin to Rac1 revealed FLNa and IQGAP1 as putative links between β1 integrin and Rac1 (Fig. 1A). Both FLNa and IQGAP1 were confidently identified in all three studies. Therefore, we tested the hypothesis that FLNa and IQGAP1 contribute to integrin-modulated Rac1 activity.

To assess the contribution of FLNa and IQGAP1 to Rac1 activation, mouse embryonic fibroblasts (MEFs) (Fig. 1B) and human U2OS osteosarcoma cells (Fig. 1C) were plated on FN, subjected to siRNA-mediated knockdown using different targeting oligos, and levels of GTP-Rac1 were measured by effector pull-down. Non-targeting-siRNA-treated MEFs exhibited a transient wave of Rac1 activity during spreading on FN, with a peak of activity observed at 45 minutes (Fig. 1D,E) (Bass et al., 2007; Humphries et al., 2009). By contrast, suppression of either FLNa or IQGAP1 expression resulted in enhanced and sustained Rac1 activation (Fig. 1D,E). Similarly, silencing of either FLNa or IQGAP1 expression in human osteosarcoma cells resulted in enhanced Rac1 activity during spreading on FN (Fig. 1F). These data indicate that both FLNa and IQGAP1 play an important role in suppressing Rac1 activity downstream of FN engagement.

Integrins undergo conformational regulation that determines their activation state and ligand-binding competency. Proteomic analyses suggested that FLNa and IQGAP1 were specifically enriched to adhesion complexes upon FN engagement (Fig. 1A). As both FLNa and IQGAP1 have been reported to co-immunoprecipitate with β1 integrin (Calderwood et al., 2001; Nakajima et al., 2005), we tested the requirement for ligand engagement in the recruitment of FLNa and IQGAP1 to β1 integrin. FLNa and IQGAP1 did not co-precipitate with β1 integrin in cells in suspension, but were found in complexes with β1 integrin when cells adhered and spread on FN (Fig. 1G). The recruitment of FLNa and IQGAP1 to β1 integrin increased with time as cells spread on FN (Fig. 1G), and correlated with Rac1 inactivation (Fig. 1D,E). As the kinetics of FLNa and IQGAP1 recruitment to β1 integrin correlated with the inactivation of Rac1 (Fig. 1G), and as suppression of FLNa and IQGAP1 expression resulted in elevated and sustained Rac1 activity (Fig. 1D,E), we hypothesised that FLNa and IQGAP1 might cooperate to constrain Rac1 activity following integrin engagement.

FLNa and IQGAP1 form a complex at sites of integrin activation

To test if FLNa and IQGAP1 cooperate to constrain Rac1 activity, we initially assessed whether they were part of the same protein complex in cells. Reciprocal co-immunoprecipitation experiments demonstrated an association between FLNa and IQGAP1 (Fig. 2A). By contrast CD98hc, a protein enriched in FN-induced adhesion complexes that links β1 integrin to another small GTPase, Arf6 (Humphries et al., 2009), did not co-immunoprecipitate with either FLNa or IQGAP1 (Fig. 2A). To complement immunoprecipitation analyses, the subcellular distribution of FLNa and IQGAP1 was assessed. FLNa and IQGAP1 demonstrated substantial co-localisation with each other (Fig. 2B,C) and with the adhesion complex protein paxillin in cells plated on FN (Fig. 2C). These data suggest that FLNa and IQGAP1 associate, either directly or indirectly, at the leading edge to regulate Rac1 activity.

As FLNa and IQGAP1 co-purified with β1 integrin upon FN engagement (Fig. 1G), we studied the role of integrin activation in the formation of the FLNa–IQGAP1 complex. Anti-β1 integrin antibodies that induce different integrin activation states (Byron et al., 2009) were used to dictate the conformation of integrins on the surface of cells. MEFs expressing human β1 integrin–GFP (Fig. 2D) and U2OS cells expressing FLNa–RFP and IQGAP1–GFP (Fig. 2E) were allowed to spread on immobilised 12G10 (a mouse anti-human monoclonal antibody that induces a high affinity, activated conformation of β1 integrin) or 4B4 (a mouse anti-human monoclonal antibody that induces a low affinity, inactive conformation of β1 integrin). Extensive co-localisation of FLNa and IQGAP1 was observed in the lamellipodia of cells with active β1 integrins but not inactive β1 integrins (Fig. 2D,E). This finding suggests that integrin activation regulates the subcellular distribution of FLNa and IQGAP1.

To analyse further the relationship between integrin activation and FLNa–IQGAP1 complex formation, β1 integrin was immunoprecipitated using activation-state-specific anti-β1 integrin antibodies (Fig. 3A). FLNa, IQGAP1 and talin, a protein that associates with high affinity integrin (Tadokoro et al., 2003), co-purified with active β1 integrin but not with inactive β1 integrin or transferrin receptor (Fig. 3A). Given that FLNa and IQGAP1 co-localise when cells are plated on activating anti-integrin antibodies and co-purify with active β1 integrin, we tested whether integrin activation controls the localisation of the FLNa–IQGAP1 complex. Micropatterned surfaces were fabricated to immobilise conformation-specific anti-β1 integrin antibodies and therefore spatially constrain integrin conformation. Both IQGAP1–GFP and FLNa–RFP were specifically recruited and enriched to sites of integrin activation but not to regions of integrin inactivation (Fig. 3B). To test if either FLNa or IQGAP1 were necessary to recruit the complex to active β1 integrin, assays were performed with cells depleted of FLNa or IQGAP1. Suppression of either FLNa or IQGAP1 expression was sufficient to substantially reduce the recruitment of both proteins to anti-active β1 integrin antibody-coated patches (Fig. 3B) and to reduce co-purification with active β1 integrin (Fig. 3C). These data indicate that both FLNa and IQGAP1 are necessary to recruit the complex to active β1 integrin. Taken together, these findings led us to postulate that integrin engagement initially triggers the activation of Rac1 followed by the dynamic recruitment of a complex containing FLNa and IQGAP1 that serves to reduce Rac1 activity and prevent dysregulated Rac1 signalling. This is consistent with the fact that the FLNa–IQGAP1 complex does not localise to focal adhesions, which are sites of integrin activation (Askari et al., 2010), but instead to lamellipodia, at early adhesion structures (Fig. 2C), which are sites of dynamic Rac1 activation (Machacek et al., 2009).

IQGAP1 recruits RacGAP1 to suppress Rac1 activity

FLNa and IQGAP1 have been reported to bind directly to Rac1 (Kuroda et al., 1996; Ohta et al., 1999); however, these proteins lack intrinsic GAP activity (Ho et al., 1999). Therefore, we hypothesised that FLNa and IQGAP1 could modulate Rac1 activation through the recruitment of additional GTPase activity modulators. To identify new FLNa and IQGAP1 binding partners, GFP pull-downs were performed in cells transiently expressing FLNa–GFP, IQGAP1–GFP, Rac1–GFP, RCC2–GFP or GFP alone and co-purifying associated proteins were identified by mass spectrometry (MS) (Fig. 4A–C). GFP and RCC2–GFP, a protein previously reported to regulate Rac1 activity (Humphries

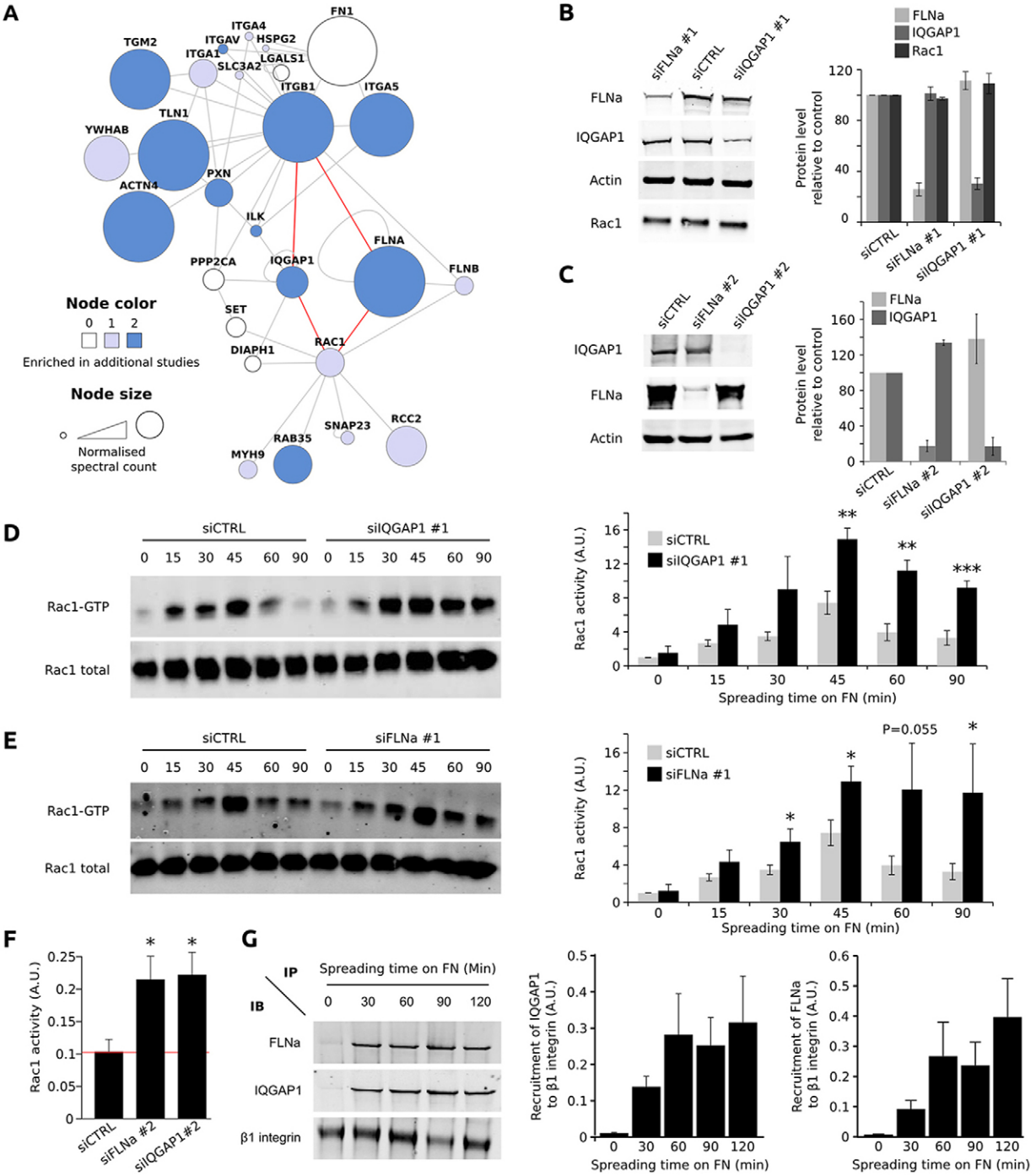

Fig. 1. FLNa and IQGAP1 suppress integrin-mediated Rac1 activation. (A) The network of FN-induced adhesion complexes that connect β1 integrin to Rac1. Proteins identified in FN-induced adhesion complexes (Humphries et al., 2009) were mapped onto a literature-curated PPI network (see the Materials and Methods for details). Each node (circle) represents a protein (labelled with gene name) and each edge (line) represents a reported interaction between two proteins. Node colour indicates whether a particular protein was also identified by Kuo et al. (Kuo et al., 2011) and/or Schiller et al. (Schiller et al., 2011). Node area is proportional to the normalised spectral count of the proteins identified by Humphries et al. (Humphries et al., 2009). Reported direct binders of β1 integrin and Rac1 are displayed, and red edges highlight selected putative links between β1 integrin and Rac1. To allow a clear visualisation of the connection between β1 integrin and Rac1, nodes of this network were manually organised. (B–F) To study the role of FLNa and IQGAP1 in Rac1 activation, MEFs (B) and U2OS cells (C) were treated with control oligonucleotide (siCTRL) or siRNA targeting FLNa or IQGAP1, and Rac1 activity was measured using an effector pull-down approach (D–F). (D,E) Rac1 activation level in MEFs was measured during cell spreading on FN and Rac1 activity was normalised to that of siCTRL cells kept in suspension (siFLNa #1 $n=6$; siIQGAP1 #1 $n=4$). (F) Rac1 activation levels in U2OS cells, knocked down for FLNa or IQGAP1 was measured after 1 hour of spreading on FN ($n=4$). (G) Quantification of FLNa and IQGAP1 recruitment to β1 integrin during cell spreading on FN. For each time point, total β1 integrin was immunoprecipitated from HFF cell lysates using the pan-β1-integrin antibody K20 and analysed by western blotting ($n=4$). The kinetics of FLNa and IQGAP1 recruitment to β1 integrin were normalised to the amount of β1 integrin. Error bars represent s.e.m. (*$P<0.05$; **$P<0.01$; ***$P<0.005$). AU, arbitrary unit; IB, immunoblot; IP, immunoprecipitation.

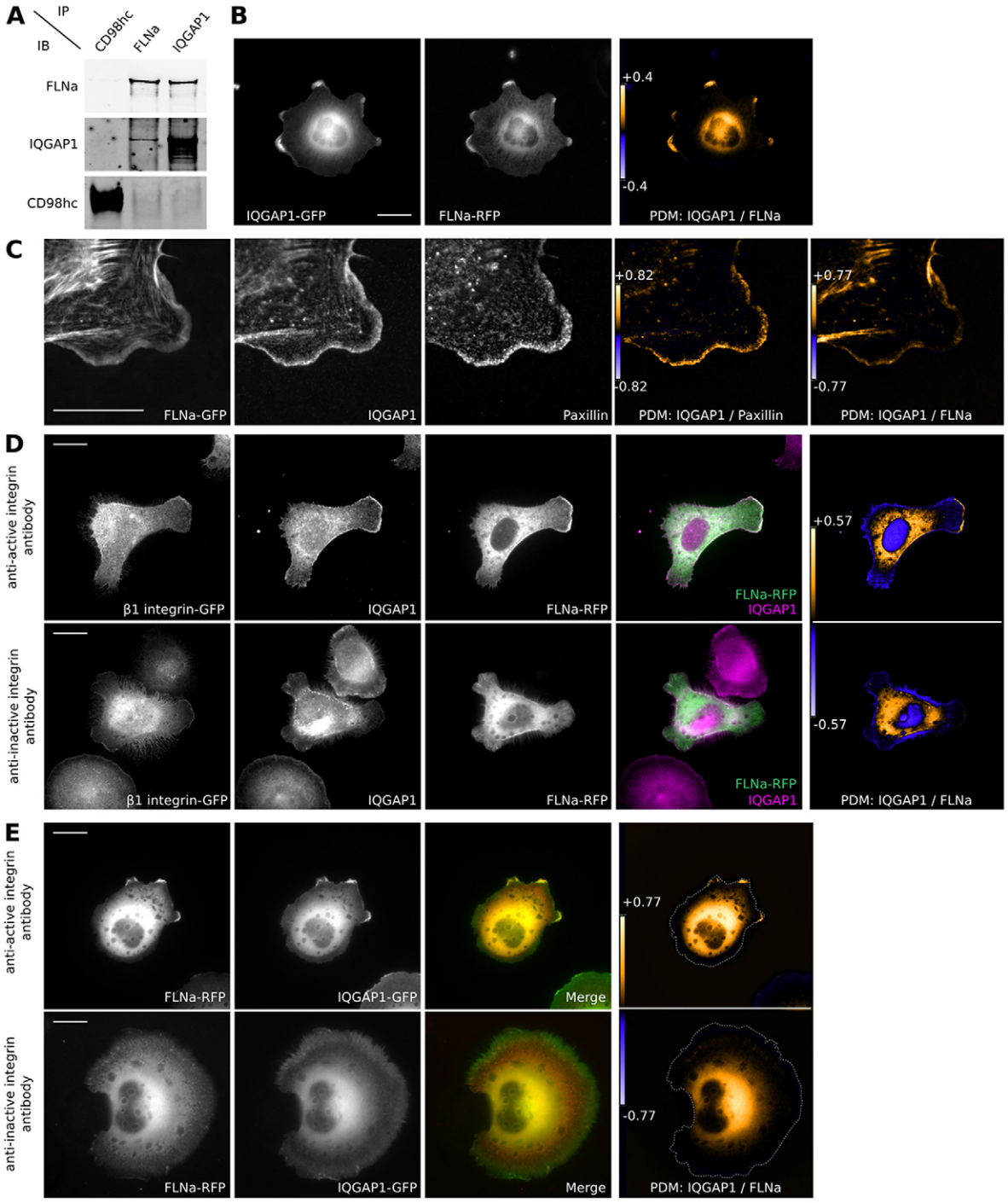

Fig. 2. FLNa and IQGAP1 form a complex. (A) Co-association of FLNa and IQGAP1 was assessed by immunoprecipitation from HFF cell lysates following spreading on FN (n=3). (B) Co-localisation of FLNa and IQGAP1 was determined by fluorescence microscopy in U2OS cells expressing IQGAP1–GFP and FLNa–RFP, plated on FN for 2 hours. PDM (product of the differences from the mean) images were created by calculating and displaying the PDM value for each pixel, where PDM=(red intensity−mean red intensity)×(green intensity−mean green intensity). (C) Co-localisation of FLNa, IQGAP1 and paxillin was determined by fluorescence microscopy in 3T3 cells expressing FLNa–GFP, plated on FN for 2 hours. (D,E) Subcellular localisation of FLNa and IQGAP1 was analysed in human β1-integrin–GFP-expressing MEFs (D) transiently expressing FLNa–RFP and in U2OS cells (E) transiently expressing IQGAP1–GFP and FLNa–RFP, plated on anti-β1 integrin monoclonal antibodies that induce different integrin activation states (12G10, active; 4B4, inactive). Images are representative of all cells plated on anti-integrin antibodies. Scale bars: 10 μm (C); 20 μm (B,E); 25 μm (D).

et al., 2009), were used as controls. In total, 1371 proteins were detected in the five pull-downs (supplementary material Table S1). Following normalisation and specificity validation against the GFP and RCC2–GFP controls, 141, 122 and 408 proteins were identified as specifically enriched to FLNa–GFP (supplementary material Table S2), IQGAP1–GFP (supplementary material

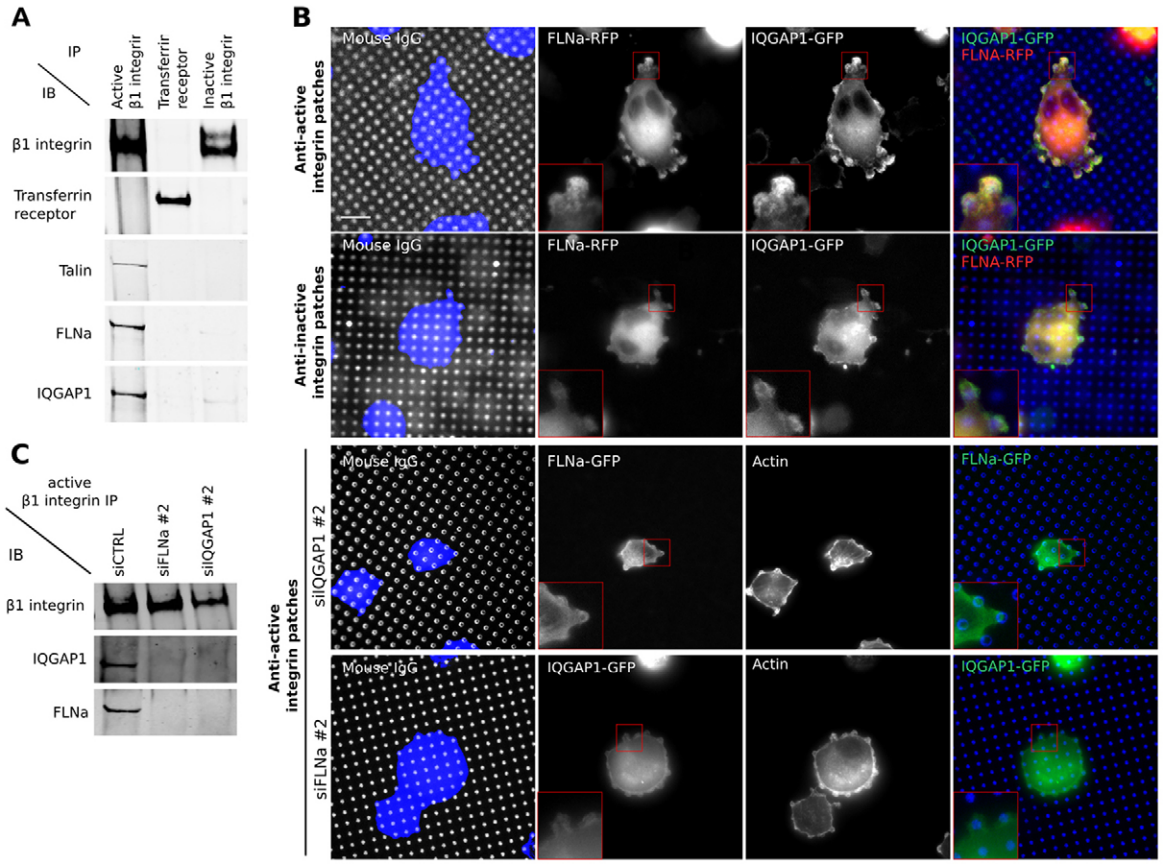

Fig. 3. FLNa and IQGAP1 are recruited to active integrins. (A) β1 integrin was immunoprecipitated from HFF cell lysates using activation-state-specific anti-β1-integrin antibodies (9EG7, active; mAb13, inactive) and anti-transferrin-receptor antibody (OKT9) as a negative control ($n=4$). (B) U2OS cells transiently expressing FLNa–RFP and IQGAP1–GFP were plated on anti-β1-integrin antibody-coated patches (12G10, active; 4B4, inactive), and U2OS cells transiently expressing FLNa–GFP or IQGAP1–GFP and knocked down for either FLNa or IQGAP1 were plated on 12G10 patches. (C) The recruitment of FLNa and IQGAP1 to active β1 integrins was assessed by immunoprecipitation using 9EG7 from U2OS cells, in which either FLNa or IQGAP1 was knocked down. IB, immunoblot; IP, immunoprecipitation. Scale bar: 10 μm.

Table S3) and Rac1–GFP (supplementary material Table S4), respectively. These datasets were integrated with PPI databases to construct a network-based view of the FLNa–IQGAP1–Rac1 complex (Fig. 4C). As a validation of this approach, many known binding partners of the bait proteins were identified (Fig. 4C). For example, refilin B (Gay et al., 2011) and R-Ras (Griffiths et al., 2011) were identified in the FLNa–GFP pull-down; calmodulin (Ho et al., 1999), Rac1 and Cdc42 (Bashour et al., 1997) in the IQGAP1–GFP pull-down; and RhoGDI (Chuang et al., 1993) in the Rac1–GFP pull-down (supplementary material Tables S2–S4). Interestingly, FLNa was found to be weakly enriched in the IQGAP1–GFP pull-downs and IQGAP1 was detected but not enriched in the FLNa–GFP pull-downs (supplementary material Table S1). These observations might suggest that the IQGAP1–FLNa association is not direct.

To highlight proteins detected by MS that may have putative roles in the regulation of Rac1, Gene Ontology analysis was used to identify proteins annotated with the term ‘GTPase regulator activity’, and these proteins were hierarchically clustered using normalised spectral counts as a measure of relative protein abundance (Fig. 4B). Using this approach, two Rac1 GAPs, RacGAP1 (MgcRacGAP or CYK4) and srGAP2, were found to be specifically enriched in the IQGAP1–GFP and Rac1–GFP pull-downs, but only RacGAP1 was robustly identified in all three biological repeats (Fig. 4B). In addition, analysis of the sub-network connecting Rac1, FLNa and IQGAP1, using an algorithm that clusters nodes within a network as a function of their connectivity, revealed that RacGAP1 had a central position in this network (Fig. 4C). Surprisingly, no known Rac1 GAPs were identified in the FLNa–GFP pull-down even though such interactions have been reported previously (Ohta et al., 2006). We therefore focused on the potential interaction between IQGAP1 and RacGAP1 as a possible mechanism by which the FLNa–IQGAP1 complex might suppress Rac1 activity.

A RacGAP1–IQGAP1 association was supported by immunoblotting of GFP pull-downs of FLNa–GFP, IQGAP1–GFP and Rac1–GFP (Fig. 4D), and further validated by co-immunoprecipitation of endogenous RacGAP1 with IQGAP1 (Fig. 5A). In addition, proximity ligation assays between endogenous IQGAP1 and endogenous RacGAP1 indicated that both were in close proximity within cells (theoretical maximum distance of 30–40 nm) suggesting that these two proteins are likely to interact directly (Fig. 5B). Furthermore, although the subcellular localisation of endogenous RacGAP1 and RacGAP1–FLAG were mostly nuclear [consistent with the reported role of RacGAP1 in cell cycle regulation (Minoshima et al., 2003)], both

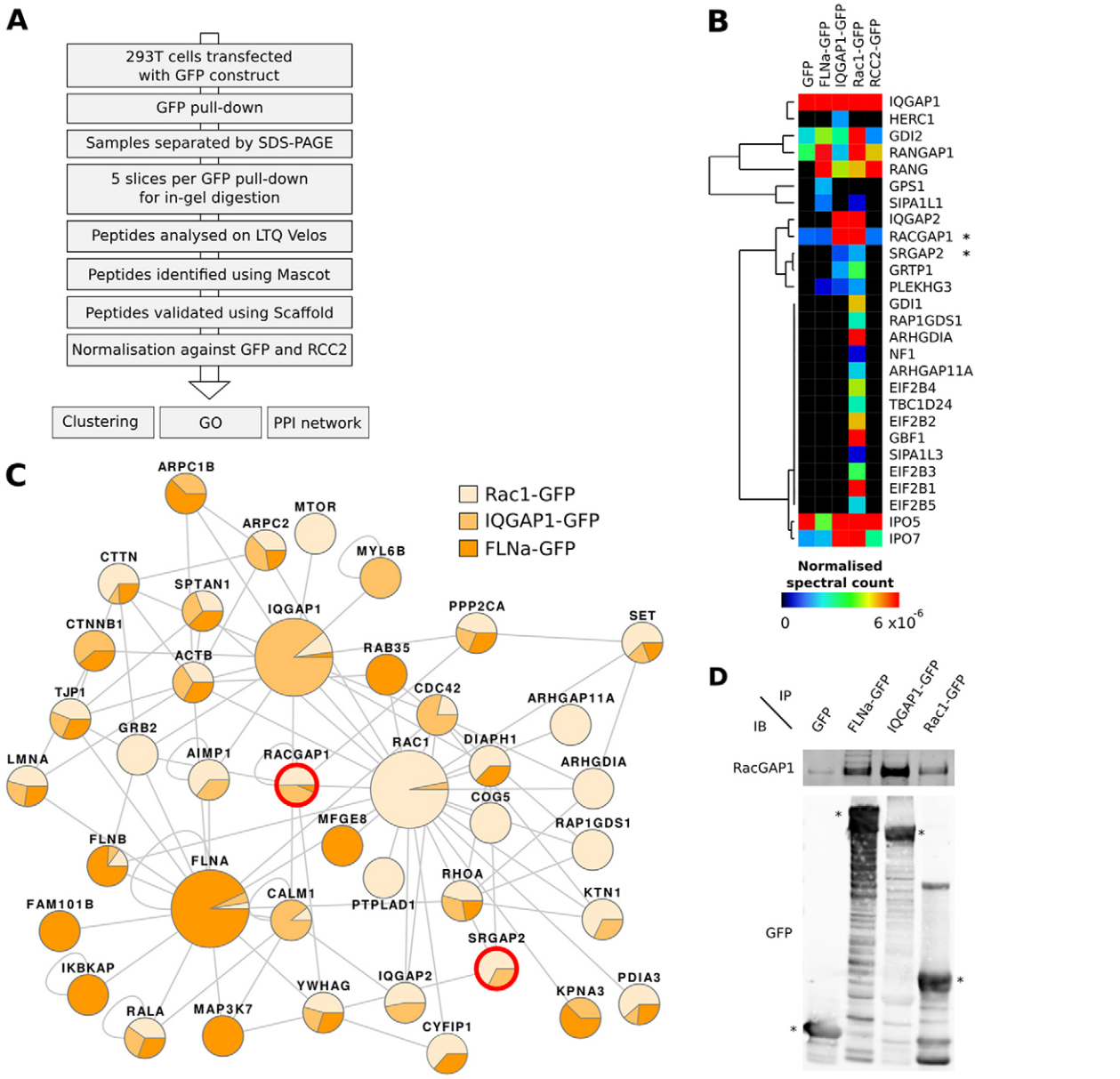

Fig. 4. MS analysis of FLNa-, IQGAP1- and Rac1-associated proteins. (A) Work-flow used to identify new FLNa, IQGAP1 and Rac1 binding partners. (B) Hierarchical clustering of proteins annotated with the Gene Ontology term 'GTPase regulator activity' identified by mass spectrometry in GFP, FLNa–GFP, IQGAP1–GFP and RCC2–GFP pull-downs. Known Rac1 GAPs are highlighted with asterisks. (C) Organic representation of the sub-network connecting FLNa, IQGAP1 and Rac1. The proteins identified by mass spectrometric analysis of the FLNa–GFP, IQGAP1–GFP and Rac1–GFP pull-downs were mapped onto a literature-based PPI network. Nodes are displayed as pie charts illustrating the relative abundance of each protein in each respective pull-down. Larger nodes represent the three bait proteins, and red node borders highlight known Rac1 GAPs. Nodes of this network were automatically organised using an algorithm that clusters nodes as a function of their connectivity. (D) Co-purification of RacGAP1 with IQGAP1–GFP was tested by western blot analysis of GFP pull-downs performed in 293T cells transiently expressing GFP, FLNa–GFP, IQGAP1–GFP or Rac1–GFP. Asterisks represent the positions of each of the GFP-tagged proteins.

endogenous RacGAP1 and RacGAP1–FLAG displayed substantial co-localisation with IQGAP1 in membrane ruffles (Fig. 5C). The membrane localisation of endogenous RacGAP1 was specific and was confirmed by the loss of membrane RacGAP1 staining in RacGAP1-knockdown cells (Fig. 5C). Importantly, suppression of IQGAP1 or FLNa expression triggered the loss of RacGAP1 localisation from membrane ruffles (Fig. 5C). All together, these data indicate that the FLNa–IQGAP1 complex recruits RacGAP1 to the cell periphery. In addition, knockdown of RacGAP1 expression triggered an increase in Rac1 activity following integrin–FN engagement (Fig. 5D). Furthermore, immunoprecipitation using activation-state-specific anti-β1 integrin antibodies revealed that RacGAP1 co-purifies only with active integrins (Fig. 5E). Since RacGAP1 exhibits functional GAP activity toward Rac1/2/3 (Bastos et al., 2012; Touré et al., 1998), these findings are consistent with a mechanism whereby the formation of a FLNa–IQGAP1 complex, at sites of integrin activation, functions to recruit RacGAP1 and constrain Rac1 activity.

As FLNa and IQGAP1 co-purified with β1 integrin upon FN engagement (Fig. 1G), and as the FLNa–IQGAP1

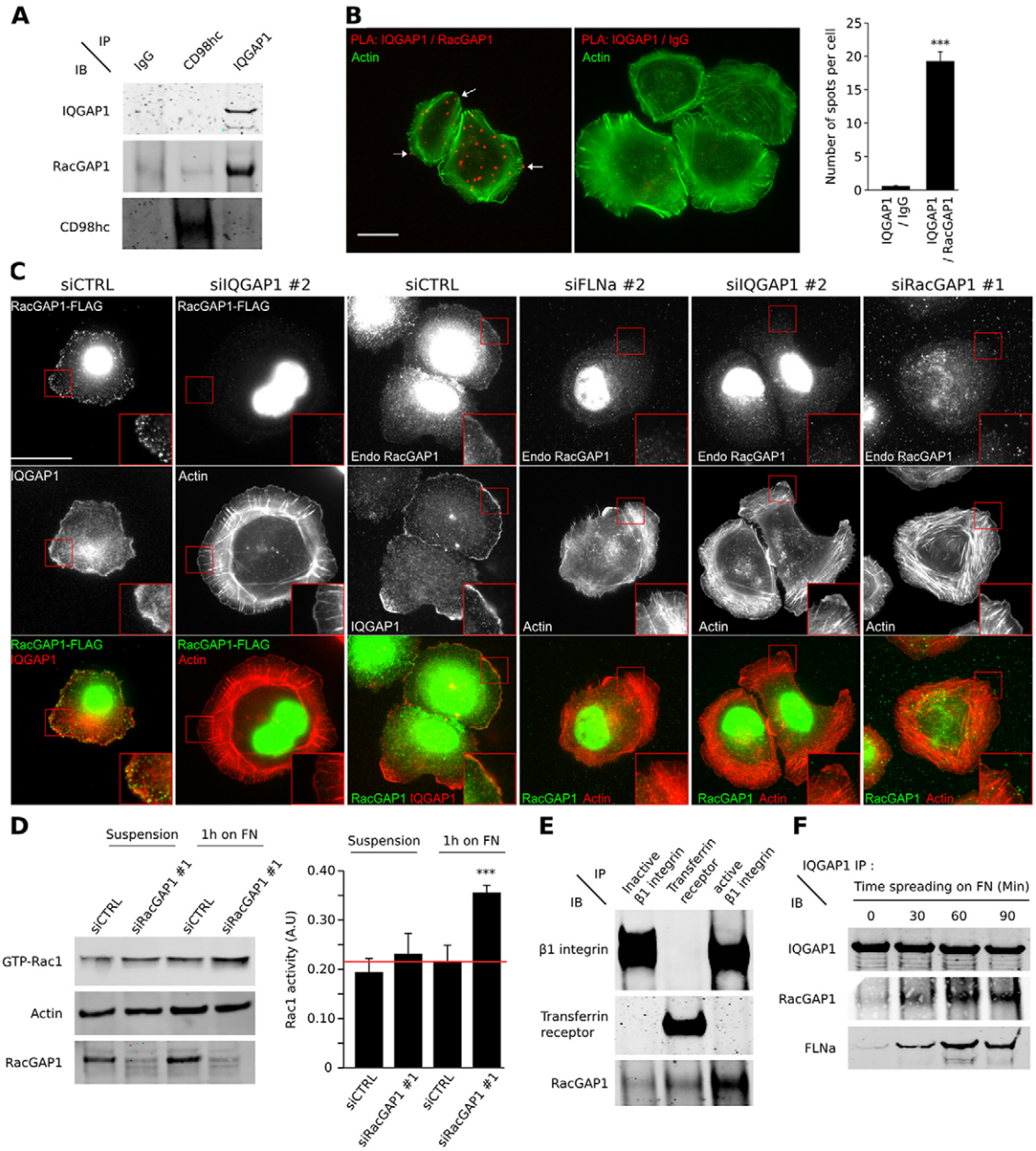

Fig. 5. RacGAP1 is recruited to IQGAP1 to suppress Rac1 activity. (A) Co-purification of endogenous IQGAP1 and RacGAP1 was assessed by immunoprecipitation in U2OS cells plated on FN. (B) Direct association between endogenous IQGAP1 and endogenous RacGAP1 was assessed by proximity ligation assay (PLA) in U2OS cells plated on FN for 1 hour. PLAs were quantified by counting the number of positive spots per cell using ImageJ (PLA IQGAP1/RacGAP1 $n=70$; PLA IQGAP1/IgG $n=79$). Arrows highlight the positive spots at the cell periphery. (C) Subcellular location of RacGAP1 (endogenous or RacGAP1–FLAG) and IQGAP1 was analysed in siCTRL-, siFLNa-, siIQGAP1- or siRacGAP1-treated U2OS cells plated on FN for 1 hour. (D) Rac1 activation levels in RacGAP1 siRNA-treated U2OS cells spread on FN for 1 hour or kept in suspension were measured by effector pull-down and analysed by western blotting ($n=5$). Error bars represent s.e.m. (***$P<0.005$). (E) The recruitment of RacGAP1 to β1 integrin was assessed by immunoprecipitation from HFF cell lysates using activation-state-specific anti-β1-integrin antibodies (9EG7, active; mAb13, inactive) and anti-transferrin-receptor antibody (OKT9) as a negative control. (F) The kinetics of FLNa and RacGAP1 recruitment to IQGAP1 were assessed by immunoprecipitation in U2OS cells during cell spreading on FN. IB, immunoblot; IP, immunoprecipitation; PLA, proximity ligation assay. Scale bars: 20 µm (B); 25 µm (C).

complex was found to recruit RacGAP1 to the cell periphery, we tested the requirement for ligand engagement in the assembly of the FLNa–IQGAP1–RacGAP1 complex (Fig. 5F). FLNa and RacGAP1 co-precipitated with IQGAP1 only when cells were adhered and spread on FN (Fig. 5F). The recruitment of FLNa and RacGAP1 to IQGAP1 increased as cells spread on FN (Fig. 5F), correlating with Rac1 inactivation (Fig. 1D,E) and with FLNa and IQGAP1 recruitment to β1 integrin (Fig. 1G). Taken together, these data demonstrate that a FLNa–IQGAP1–RacGAP1 complex assembles at β1 integrin activation sites, during cell spreading on FN, to suppress Rac1 activity.

FLNa, IQGAP1 and RacGAP1 regulate Rac1 activity, membrane protrusion dynamics and directional cell migration

FLNa, IQGAP1 and RacGAP1 were demonstrated to modulate Rac1 activity during cell spreading on FN by using an effector pull-down approach (Fig. 1; Fig. 5D). To validate these findings further, the activation state of Rac1 was monitored using a Rac1-Raichu probe by fluorescence lifetime microscopy (FLIM), in live cells previously knocked down for FLNa, IQGAP1 or RacGAP1 (Fig. 6A,C,E) (Itoh et al., 2002). To rule out possible off-target effects, these experiments were performed using three individual siRNA oligos targeting FLNa and IQGAP1 and two individual siRNA oligos targeting RacGAP1 (Fig. 6B,D). In comparison with control-treated cells, suppression of FLNa, IQGAP1 or RacGAP1 expression resulted in lower lifetime of the Rac1-Raichu probe, in both

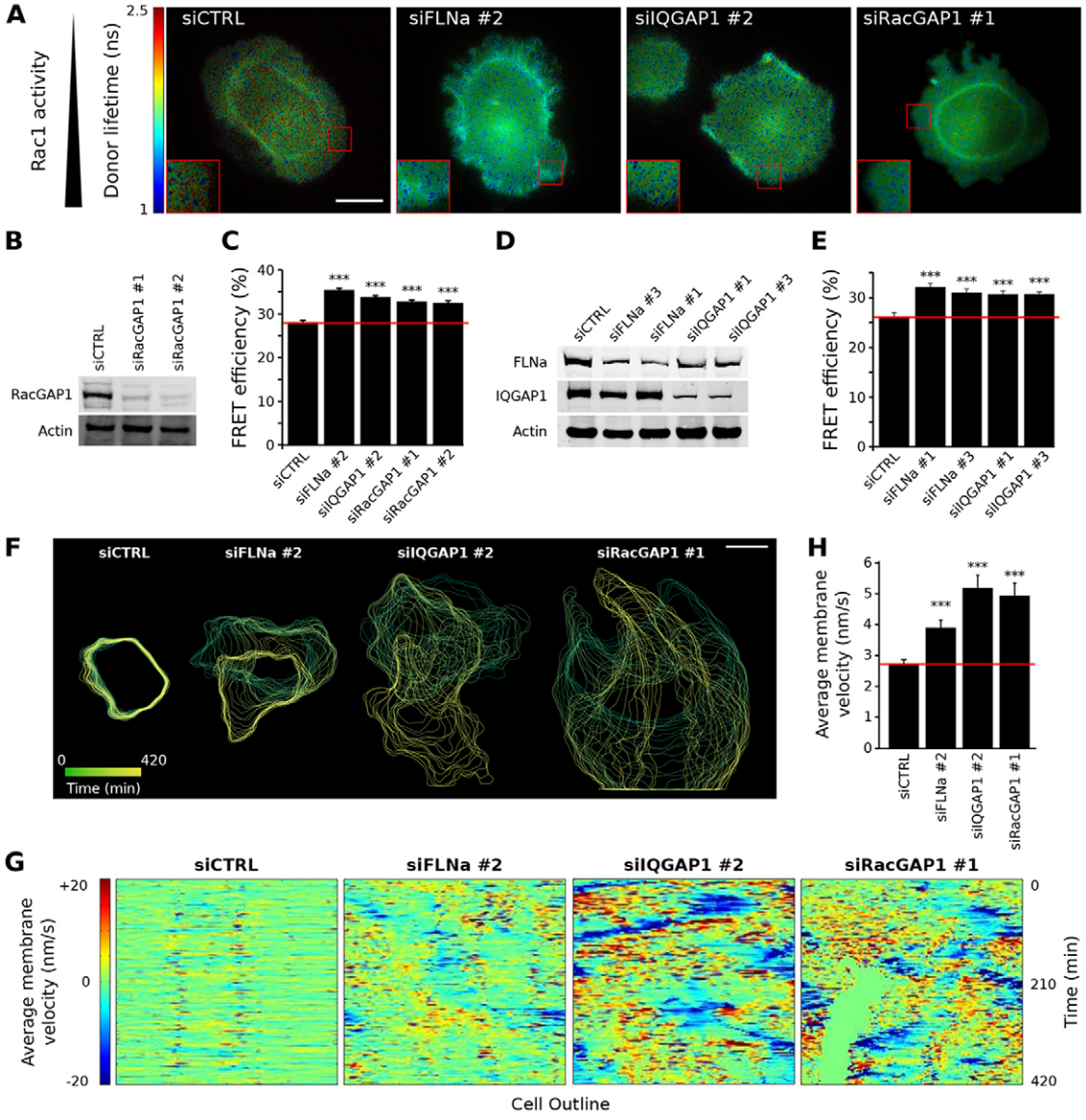

Fig. 6. FLNa, IQGAP1 and RacGAP1 regulate Rac1 activity and membrane protrusion dynamics. (A–E) Activation state of Rac1 was monitored using the Rac1-Raichu probe in U2OS cells (A–C) and 3T3 cells (D,E), pre-treated with control oligonucleotide (siCTRL) or siRNA targeting FLNa (siFLNa #1 and #3 in 3T3 cells; siFLNa #2 in U2OS cells), IQGAP1 (siIQGAP1 #1 and 3 in 3T3 cells; siIQGAP1 #2 in U2OS cells) or RacGAP1 (siRacGAP1 #1 and #2 in U2OS cells), plated on FN for 1 hour. Rac1 activity was quantified by measuring the average donor lifetime of the Raichu probe across the whole cell (low lifetime, high activity; high lifetime, low activity) using FLIM/FRET (U2OS cells, siCTRL $n=73$, siIQGAP1 #2 $n=63$, siFLNa #2 $n=63$, siRacGAP1 #1 $n=58$, siRacGAP1 #2 $n=47$; 3T3 cells, siCTRL $n=25$, siIQGAP1 #1 $n=27$, siIQGAP1 #3 $n=22$, siFLNa #1 $n=30$, siFLNa #3 $n=31$). (C,E) FRET efficiency was calculated as described in the Materials and Methods. (F-H) U2OS cells transiently expressing Lifeact-mEGFP were transfected with siCTRL, siFLNa, siIQGAP1 or siRacGAP1 and plated on FN for 4 hours. Cells were imaged for 420 minutes at 1 frame every 180 seconds. For each time point, cell outlines were segmented into 400 nodes connected by edges using QuimP11, and the velocity of each node was calculated. For each condition, the time projection (F) and motility map (G) of the cell outlines were plotted. Positive motility values (red) represent areas of membrane protrusion, whereas negative motility values (blue) represent areas of membrane retraction. (H) The overall membrane dynamics were calculated as the mean motility of the cell outline over the recording period in siCTRL ($n=34$), siFLNa ($n=27$), siIQGAP1 ($n=22$) and siRacGAP1 ($n=19$) cells. Error bars represent s.e.m. (***$P<0.005$). Scale bars: 20 μm (A,F).

human and mouse cell lines, indicating higher Rac1 activation (Fig. 6A,C,E). These data are consistent with results obtained previously, using effector pull-down assays (Fig. 1D,E; Fig. 5D), and demonstrate that FLNa, IQGAP1 and RacGAP1 are involved in suppressing Rac1 activity during cell spreading on FN.

Rac1 has a central role in regulating cell membrane protrusion during directional cell migration (Pankov et al., 2005; Wu et al., 2009). Having identified a mechanism whereby FLNa, IQGAP1 and RacGAP1 cooperate to regulate Rac1 activity, we investigated the role of these molecules in regulating cellular protrusion and migration. To assess actin dynamics and membrane protrusive activity by live-cell microscopy, FLNa, IQGAP1 or RacGAP1 expression was knocked down in U2OS cells transiently transfected with Lifeact-mEGFP (supplementary material Movies 1–4). For each condition, cell outlines were tracked (Fig. 6F) and membrane velocity measured (Fig. 6G) and quantified (Fig. 6H) using QuimP11 (Tyson et al., 2010). Consistent with increased Rac1 activity, suppression of FLNa, IQGAP1 or RacGAP1 expression enhanced membrane protrusive activity (Fig. 6F–H and supplementary material Movies 1–4) compared with control cells.

Given that FLNa, IQGAP1 and RacGAP1 suppress membrane protrusion, we next investigated whether these proteins also regulate cell migration. FLNa, IQGAP1 and RacGAP1 expression was knocked down in U2OS cells (Fig. 7A–D), and FLNa and IQGAP1 were knocked down either individually or together in MEFs (Fig. 7E,F), and migration on cell-derived matrices (CDMs) was assessed. Non-targeting-siRNA-treated cells migrated in a directionally persistent manner on CDMs (Fig. 7C,E) (Pankov et al., 2005). However, siRNA-mediated suppression of FLNa, IQGAP1 or RacGAP1 expression, in both MEFs and U2OS cells, triggered a decrease in directional migration (Fig. 7C,E) accompanied by a concomitant increase in cell speed (Fig. 7D,F). The loss of persistent migration is consistent with the observed elevation of Rac1 activity (Fig. 1D–F) and the consequent increase in protrusive activity in cells plated on FN (Fig. 6A–C) or CDMs (Fig. 7A) (Bass et al., 2007; Pankov et al., 2005). Combined suppression of both FLNa and IQGAP1 expression did not further decrease directionality or increase cell speed, suggesting that these proteins cooperate in regulating cell migration (Fig. 7E,F). These data indicate that FLNa, IQGAP1 and RacGAP1 play a fundamental role in regulating cell migration by regulating both cell directionality and cell speed.

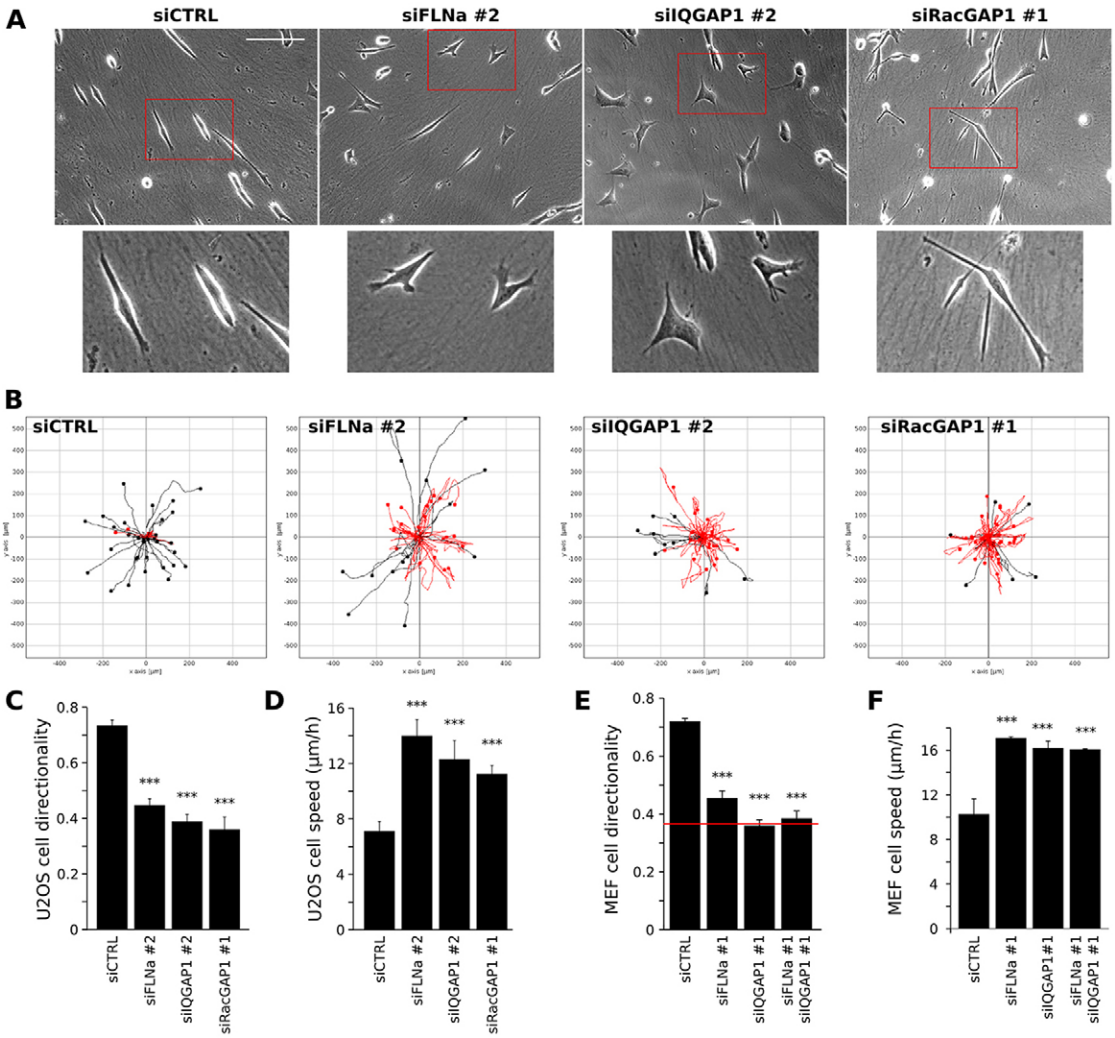

Fig. 7. FLNa, IQGAP1 and RacGAP1 regulate directional cell migration. (A–D) U2OS cells transfected with siCTRL, siFLNa, siIQGAP1 or siRacGAP1 were plated on CDMs for 4 hours and their migration recorded for 16 hours and manually tracked. (A) Representative fields demonstrating the morphology of the cells on CDMs. Red boxes delineate inset areas. For each condition, spider plots (40 cell tracks; red tracks highlight cells with directionality below 0.5) were created (B), and cell directionality (C) and cell speed (D) were analysed (n=3). (E,F) MEFs transfected with siCTRL, siFLNa, siIQGAP1 or siFLNa/siIQGAP1 were plated on CDM for 4 hours and their migration recorded for 16 hours. For each condition, cell directionality (E) and cell speed (F) were analysed (n=3). Error bars represent s.e.m. (***P<0.005). Scale bar: 20 µm.

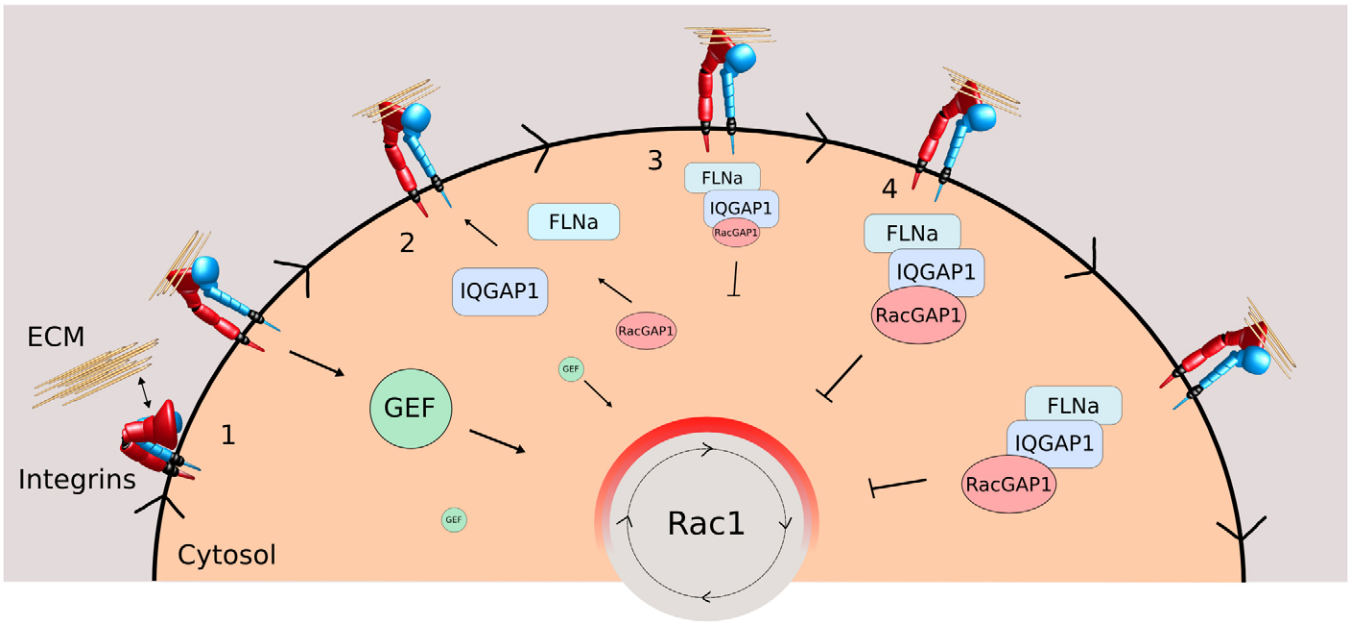

Fig. 8. Recruitment of FLNa, IQGAP1 and RacGAP1 to active β1 integrin regulates Rac1 activity. Scheme representing a cycle of sequential integrin-mediated signalling events regulating Rac1 activation. Integrin–ECM engagement triggers an increase in Rac1 activity, most likely via the recruitment of a GEF (1). Rac1 activity levels increase to a maximum, and FLNa and IQGAP1 are recruited (2 and 3). FLNa and IQGAP1 recruit RacGAP1 to suppress Rac1 activity (3 and 4). Rac1 activation level is represented by a red gradient around its edge. Hypothetical activation and protein level of GEFs and GAPs are represented by the size of their nodes.

Discussion

We have identified a novel mechanism that coordinates Rac1 activity downstream of β1 integrin activation. This conclusion is based on the following major findings: (1) FLNa and IQGAP1 are part of a complex that forms downstream of β1 integrin activation; (2) FLNa and IQGAP1 suppress Rac1 activity following FN-integrin engagement; (3) IQGAP1 recruits RacGAP1 to suppress Rac1 activity; (4) Knockdown of FLNa, IQGAP1 and RacGAP1 disrupts membrane protrusion and directional cell migration. Thus, our data suggest a model whereby integrin engagement, followed by FLNa, IQGAP1 and RacGAP1 recruitment, maintains tight control over Rac1 activity and thereby coordinates directional cell migration (Fig. 8).

Accumulating evidence indicates that IQGAP1 can function to regulate the activity of small GTPases both positively and negatively (Bashour et al., 1997; Casteel et al., 2012; Jeong et al., 2007). To date, studies of IQGAP1-dependent Rac1 activity modulation have focused primarily on the response triggered by growth factors or cytokines (Brown and Sacks, 2006; David et al., 2011; Hu et al., 2009). This is the first report to describe the essential role that cell–ECM engagement plays in IQGAP1-dependent modulation of Rac1 activity, and in contrast to stimulation with soluble extracellular cues, we show that this mechanism suppresses Rac1 activity.

IQGAP1 contains an inactive RasGAP domain and does not act directly as either a GEF or a GAP (Hart et al., 1996; Ho et al., 1999), so the precise mechanism by which IQGAP1 regulates Rac1 activity is unclear. It has been suggested that binding of Cdc42 to IQGAP1 inhibits Cdc42 intrinsic GTPase activity *in vitro*, prolonging Cdc42 activation (Hart et al., 1996; Ho et al., 1999). Thus, it was proposed that IQGAP1-mediated potentiation of Rac1 activity could occur through a similar mechanism (Brown and Sacks, 2006). Here, we report, for the first time, that IQGAP1 can also suppress Rac1 activity and we have identified RacGAP1 as the negative regulator of Rac1 that is recruited by IQGAP1. Consistent with our model, others have reported that IQGAP1 binds preferentially to GTP-Rac1 (Kuroda et al., 1996), suggesting that IQGAP1 might immobilise active Rac1 at sites of integrin activation and subsequently recruit RacGAP1 to promote GTP hydrolysis. Consistent with IQGAP1 suppressing Rac1 activity, a recent study reported that IQGAP1 promoted RhoA activation (Casteel et al., 2012), a well-established antagonist of Rac1 activity (Guilluy et al., 2011). Proteomic analyses of IQGAP1-associated proteins identified a putative RhoA GEF, namely pleckstrin homology domain-containing family G member 3, which could be involved in IQGAP1-mediated activation of RhoA (Fig. 4B and supplementary material Table S3). In addition to Rac1 and RhoA, there is evidence that IQGAP1 can recruit and regulate other small GTPases including Cdc42 (Bashour et al., 1997; Kuroda et al., 1996), Arf6 (Hu et al., 2009) and Rap1 (Awasthi et al., 2010; Jeong et al., 2007) and their downstream effectors (supplementary material Table S3) (Noritake et al., 2004; Pelikan-Conchaudron et al., 2011; Sakurai-Yageta et al., 2008). A recurring theme from these studies, and from ours, is that modulation of GTPase activity by IQGAP1 is due to the recruitment of other proteins. Therefore, it is tempting to speculate that IQGAP1 could act as a ‘small GTPase scaffolding platform’, recruiting both small GTPase regulators and effectors to the leading edge, to orchestrate cell behaviour precisely. Given that different extracellular stimuli can promote both Rac1 activation and inhibition, via IQGAP1, it is likely that the mechanisms by which IQGAP1 coordinates GTPase activity will be exquisitely dependent on both micro environmental and

cellular context. The next challenge will be to determine if these molecules are recruited to IQGAP1 simultaneously or at discrete subcellular locations and/or time, and to identify how the convergence of intracellular signals downstream of other receptors, such as growth factor receptors or syndecans, and/or post-translational modifications dictate the differential recruitment of these GTPase regulators and effectors to IQGAP1.

RacGAP1, as part of the centralspindlin complex, has been described previously to play a regulatory role during cytokinesis (Hirose et al., 2001; Minoshima et al., 2003; Oceguera-Yanez et al., 2005; Zhao and Fang, 2005). Interestingly, FLNa, IQGAP1 and Rac1 have also been reported to be important for cell division (Canman et al., 2008; Eng et al., 1998; Mondal et al., 2012; Padmanabhan et al., 2011). In addition, cytokinesis regulators and spindle components such as septins (isoforms 2 and 11) (Estey et al., 2010), calmodulin (Yu et al., 2005), kinesin-like proteins (KIF11 and KIF23) (Lee et al., 1995) and cohesin (subunits SA-1 and SA-2) (Hauf et al., 2001) were identified by mass spectrometry in the FLNa–GFP, IQGAP1–GFP and Rac1–GFP pull-downs (supplementary material Table S1). The possibility that the pathway described here could play a role in cell division will be the subject of future investigations.

Our data demonstrated that RacGAP1 plays an important role in regulating Rac1 activity at the cell leading edge during interphase. Recent work has also identified an interphase role for RacGAP1 at cell–cell junctions (Ratheesh et al., 2012). These reports of cytokinesis- and centralspindlin-independent RacGAP1 functions suggest that RacGAP1 has a broader range of functions than previously anticipated. In this context, IQGAP1 is known to localise at cell–cell junctions (Krishnan et al., 2012; Lehtonen et al., 2005; Noritake et al., 2004) and cell–cell junction proteins were identified as IQGAP1-associated proteins (e.g. β-catenin) (supplementary material Table S3). Therefore, IQGAP1 may also be involved in recruiting RacGAP1 at cell–cell junctions.

Our data demonstrated that FLNa and IQGAP1 specifically co-purified and localised with activated β1 integrin. Both IQGAP1 and FLNa have been previously reported to be recruited to β1 integrin (Calderwood et al., 2001; Kiema et al., 2006; Nakajima et al., 2005; Takahashi and Suzuki, 2006; Travis et al., 2004); however, neither FLNa or IQGAP1 localised to classical focal adhesions, which are sites of integrin activation (Askari et al., 2010), but instead to lamellipodia, at early adhesion structures (Fig. 2C). It has been reported that, in lamellipodia, unligated integrin can get activated by actin polymerisation and therefore be 'primed' to probe for adhesion sites (Galbraith et al., 2007). Therefore, it is possible that FLNa and IQGAP1 specifically target the sub-set of unligated primed integrins to restrict the formation of uncontrolled protrusions. In addition, the recruitment of FLNa to active integrin is surprising. The current model of the integrin–FLNa association would predict that FLNa binds inactive integrins. FLNa has been reported to directly bind to the β1 integrin tail (Calderwood et al., 2001; Ehrlicher et al., 2011; Travis et al., 2004), in a region overlapping with the talin binding site (Kiema et al., 2006). FLNa binding to integrin is thought to compete with talin, a key β1 integrin activator (Tadokoro et al., 2003), and therefore to inactivate integrin. However, our data demonstrated that FLNa is recruited specifically to activated integrins along with talin. Therefore, in this context we predict that the recruitment of FLNa to integrin is unlikely to be direct and one of the next challenges leading from this study will be to determine how FLNa and IQGAP1 are recruited to activated integrins.

While we discovered that RacGAP1 was recruited to a complex containing FLNa and IQGAP1 upon integrin activation, it has been reported previously that FLNa can recruit an alternative suppressor of Rac1 activity, FilGAP, and this association is modulated by mechanical strain (Ehrlicher et al., 2011; Nieves et al., 2010; Ohta et al., 2006). Although we were unable to detect the association of FilGAP with GFP–FLNa in our mass spectrometric analyses, the fact that multiple mechanisms exist to limit Rac1 activity upon integrin activation, or during integrin-mediated mechanosensation, highlights the importance of constraining Rac1 activity during these processes. Given the fundamental role that Rac1 plays in regulating actin polymerisation and cellular behaviour it is perhaps not surprising that Rac1 activity must be tightly coordinated both spatially and temporally.

Our experiments demonstrated that suppression of FLNa, IQGAP1 or RacGAP1 expression disrupted cell migration. Silencing any of these proteins not only increased the speed of migration but also triggered a loss in the ability to migrate in a directionally-persistent manner. Others have reported previously either no migratory defect (Baldassarre et al., 2009) or a decreased speed of cell migration (Leung et al., 2010) following FLNa knockdown for cells on FN. These discrepancies could be explained by the different mode of migration that cells utilise on fibrillar matrices compared to 2D FN (Petrie et al., 2009). Migration defects observed on CDM could be explained by high Rac1 activity and the concomitant increase in protrusion dynamics measured in these cells (Bass et al., 2007; Pankov et al., 2005). This is consistent with our proposed model that FLNa, IQGAP1 and RacGAP1 are recruited to newly formed protrusions in order to restrict their expansion by locally suppressing Rac1 activity. Indeed, during a protrusion event, a cell explores its environment by making new transient cell–ECM adhesions. Integrin activation at these adhesion sites results in Rac1 activation and promotion of the initial protrusion. In the absence of an off switch to break the cycle of integrin and Rac1 activation, protrusion events would become dysregulated and lack control. The recruitment of the FLNa–IQGAP1 complex to sites of integrin activation may be one mechanism whereby cell protrusion events can be spatially restricted.

In conclusion, we report a signalling pathway linking β1 integrin to Rac1 activity that controls cell migration. We envision these components as the nodes of a much broader regulatory network, integrating multiple matrix-associated and soluble signals from the microenvironment to control cell behaviour spatially. The next challenge will be to identify other components of this network, their inter-connection, and how they transduce information to regulate cell migration. It is likely that systems-level proteomic analysis of the components of this network, using IQGAP1 and FLNa binding partners as a starting point, will help to unravel the structure, the dynamics, and the regulatory mechanisms of this network.

Materials and Methods

Cell culture

Wild-type and β1-integrin–GFP-expressing MEFs were maintained in Dulbecco's modified Eagle's medium (DMEM; Sigma-Aldrich) supplemented with 10% (vol/vol) foetal calf serum (FCS; Biosera) and 20 U/ml mouse interferon γ (Sigma-Aldrich) at 33℃, 5% (vol/vol) CO_2. Human foreskin fibroblasts (HFFs), mouse 3T3 cells, human 293T embryonic kidney cells and human U2OS osteosarcoma cells were cultured in DMEM supplemented with 10% (vol/vol) FCS at 37℃, 5% (vol/vol) CO_2.

Reagents

Mouse anti-human β1 integrin monoclonal antibody, JB1A was provided by John Wilkins (University of Manitoba, Winnipeg, MB, Canada). Mouse anti-human β1 integrin monoclonal 12G10 and rat anti-human β1 integrin monoclonal 9EG7 (which recognise receptor with high affinity for ligand, termed 'active') and mAb13 (which recognises receptor with low affinity for ligand, termed 'inactive') were produced as reported previously (Mould et al., 1995; Mould et al., 1996). Function-blocking mouse anti-human β1 integrin monoclonal 4B4 was obtained from Beckman Coulter and function-neutral mouse anti-human β1 integrin monoclonal K20 was obtained from Santa Cruz Biotechnology. Other mouse monoclonal antibodies used were directed against human paxillin (clone 349; BD Biosciences), human transferrin receptor (H68.4; Invitrogen; and OKT9; European Collection of Cell Cultures), mouse and human actin (AC-40; Sigma-Aldrich), mouse IQGAP1 (K0100-3; MBL international), mouse and human Rac1 (BD Biosciences), human RacGAP1 (1G6; Sigma-Aldrich) and GFP (Roche). Polyclonal antibodies used were goat anti-human CD98hc (C20; Santa Cruz Biotechnology), rabbit anti-human IQGAP1 (H-109; Santa Cruz Biotechnology), mouse anti-human IQGAP1 (D-3; Santa Cruz Biotechnology), rabbit anti-human RacGAP1 (PA5-22265; Thermo Scientific), rabbit anti-human FLNa (H-300; Santa Cruz Biotechnology), rabbit anti-mouse FLNa (A301-133A; Bethyl Laboratories) and goat anti-human talin (C-20; Santa Cruz Biotechnology). Secondary Alexa-Fluor-647-conjugated anti-mouse and Alexa-Fluor-488-conjugated anti-rabbit antibodies were used for immunofluorescence, and Alexa-Fluor-680-conjugated or Alexa-Fluor-800-conjugated antibodies were used for western blotting; all were obtained from Invitrogen. Rabbit IgG and bovine plasma FN were obtained from Sigma-Aldrich. A codon optimised RacGAP1–FLAG was synthesised by Genscript, and cloned into the pcDNA3 vector (*Eco*RI-*Bam*HI). The following plasmids were obtained as gifts: GST-PAK-1 CRIB domain (from Kozo Kaibuchi, Nagoya University School of Medicine, Nagoya, Japan), FLNa–RFP and FLNa–GFP (from Fumihiko Nakamura, Brigham and Women's Hospital, Boston, MA), IQGAP1–eGFP (from Robert Grosse, Institute of Pharmacology, University of Marburg, Marburg, Germany), and Lifeact-mEGFP (from Roland Wedlich-Söldner, Max Planck Institute of Biochemistry, Martinsried, Germany).

Preparation of micropatterned substrates

Poly(dimethyl siloxane) (PDMS; Sylgard 184; Dow Corning) stamps with patterns (2 μm in diameter) were cast from photoresist patterned silicon wafers as described previously (Tan et al., 2004). To spatially constrain β1 integrin conformation, PDMS was inked with activation-state-specific β1 integrin antibodies (12G10, active; 4B4, inactive) at 50 μg/ml in PBS for 1 hour at room temperature. The stamps were then submerged in sterile water and dried using a stream of N_2. The stamps were placed feature-face down on PDMS-coated glass coverslips that were treated with ultraviolet ozone (Jelight Company) to transfer the patterned protein to the substrates. Finally, Pluronic F-127 (Sigma-Aldrich) was adsorbed to prevent unwarranted protein adsorption to the PDMS substrates.

siRNA knockdown

The expression of proteins of interest was reduced using 100 nM ON-TARGETplus modified siRNA (Dharmacon, Thermo Fisher) and Lipofectamine 2000 (Invitrogen) according to manufacturer's instructions. Two rounds of transfection were necessary to achieve efficient knockdown. The ON-TARGETplus non-targeting siRNA (Dharmacon) was used as a negative control. The siRNA oligos used to knock down IQGAP1 were siIQGAP1 #1 (mouse IQGAP1, J-040589-12), siIQGAP1 #2 (human IQGAP1, J-004694-06) and siIQGAP1 #3 (mouse IQGAP1, J-040589-10). The siRNA oligos used to knock down FLNa in mouse cell lines were siFLNa #1 (J-058520-20) and #3 (J-058520-18). The FLNa smart pool (L-012579-00, Dharmacon) was used to knock down FLNa in human cell lines. The siRNA oligos used to knock down RacGAP1 in human cell lines were siRacGAP1 #1 (J-008650-06) and #2 (J-008650-08). Levels of knockdown were verified by western blotting for every experiment.

Immunoprecipitation

Cells were plated on FN for 2 hours, washed with cold PBS and lysed in CSK buffer [0.5% (wt/vol) Triton X-100, 10 mM Pipes, pH 6.8, 150 mM NaCl, 150 mM sucrose, 3 mM $MgCl_2$, 10 μg/ml leupeptin, 10 μg/ml aprotinin, 0.5 mM 4-(2-aminoethyl)benzenesulfonyl fluoride hydrochloride, 2 mM Na_3VO_4]. Lysates were clarified (centrifugation at 12,000 ***g***, 4℃ for 1 minute) and incubated with antibody-coated protein G magnetic beads (1 μg of antibody per 10 μl of beads) (Dynabeads; Invitrogen) for 1 hour at 4℃. Complexes bound to the beads were isolated using magnets, washed three times with ice-cold lysis buffer and eluted in Laemmli reducing sample buffer.

Rac1 activity assay

Active Rac1 was affinity purified from lysates using an effector pull-down approach with GST-PAK beads. Cells were serum starved and maintained in suspension for 1 hour before plating on 10 μg/ml FN-coated dishes. At various times, cells were lysed in ice-cold lysis buffer [20 mM Hepes, pH 7.5, 1% (wt/vol) Igepal, 0.5% (wt/vol) sodium deoxycholate, 140 mM NaCl, 4 mM EDTA, 4 mM EGTA, 10% (wt/vol) glycerol), and lysates were clarified by centrifugation at 12,000 g, 4℃, for 1 min. Lysates were then incubated with GST-PAK beads for 1 hour at 4℃. Beads were washed three times with ice-cold lysis buffer, and active GTPase was eluted off beads by addition of Laemmli reducing sample buffer. Samples were then resolved by SDS-PAGE and analysed by western blotting.

GFP pull-downs

GFP-tagged proteins were pulled down from 293T cell lysates using GFP-Trap agarose beads (Chromotek) according to the manufacturer's instructions. 293T cells transiently expressing bait GFP-tagged protein were lysed in 0.5% (wt/vol) NP-40, 10 mM Tris-HCl, pH 7.2, 250 mM NaCl, 0.5 mM EDTA, 10% (wt/vol) glycerol, 10 μg/ml leupeptin, 10 μg/ml aprotinin, 0.5 mM 4-(2-aminoethyl)benzenesulfonyl fluoride hydrochloride, 2 mM Na3VO4. Lysates were then sonicated (3 pulses of 10 seconds; VibraCell VCX 500; Sonics & Materials) and centrifuged at 12,000 ***g*** for 5 min. Clarified lysates were incubated with GFP-Trap agarose beads for 1 hour at 4℃. Complexes bound to the beads were isolated by centrifugation, washed three times with ice-cold lysis buffer and eluted in Laemmli reducing sample buffer. GFP tags of Rac1–GFP, RCC2–GFP, FLNa–GFP and IQGAP1–GFP were all N-terminal.

SDS-PAGE and quantitative western blotting

Protein extracts were separated under denaturing conditions by SDS-PAGE (4–12% Bis-Tris gels; Invitrogen) and transferred to nitrocellulose membrane. Membranes were blocked overnight at 4℃ with blocking buffer (Sigma-Aldrich) and then incubated with the appropriate primary antibody diluted in blocking buffer (Sigma-Aldrich) for 2 hours. Membranes were washed with PBS and then incubated with the appropriate fluorophore-conjugated secondary antibody diluted 1:5000 in blocking buffer for 30 minutes. Membranes were washed in the dark and then scanned using an Odyssey infrared imaging system (LI-COR Biosciences). Band intensity was determined by digital densitometric analysis using Odyssey software (version 2.1; LI-COR Biosciences).

Plasmid transfection

MEFs were transfected using Lipofectamine PLUS reagent (Invitrogen) and U2OS cells were transfected using Lipofectamine 2000 reagent. Cells were seeded in six-well plates and allowed to reach 80% confluence prior to transfection. For Lipofectamine Plus-mediated transfections, the transfection mixture consisted of 2 μg plasmid pre-incubated for 10 minutes at room temperature with 5 μl PLUS reagent diluted in 250 μl OptiMEM and 20 μl of Lipofectamine pre-incubated for 10 minutes at room temperature with 250 μl OptiMEM. For Lipofectamine 2000-mediated transfections, the transfection mixture consisted of 4 μg plasmid diluted in 250 μl OptiMEM and 7 μl Lipofectamine 2000 pre-incubated with 250 μl OptiMEM for 5 minutes at room temperature. In each case, the transfection mixtures were then incubated for 20 minutes at room temperature. The medium was removed from cells and replaced with 500 μl of OptiMEM and the appropriate transfection mixture. Following 4 hours of incubation, the transfection mixture was removed, fresh medium was added, and transfected cells were used the following day.

293T cells were transfected using 100×polyethyleneimine reagent (Sigma-Aldrich). Cells were seeded in a 15 cm dish and allowed to reach 80% confluence prior to transfection. The transfection mixture consisted of 12 μg plasmid diluted in 500 μl OptiMEM and 54 μl 1×polyethyleneimine (diluted with 150 mM NaCl) pre-incubated with 446 μl of OptiMEM for 5 minutes at room temperature. Transfection mixtures were incubated for 20 minutes at room temperature. Medium was then removed from cells and replaced with 10 ml growth medium and the transfection mixture. Following 10 hours of incubation, the transfection mixture was removed, fresh medium was added, and transfected cells were used the following day.

Immunofluorescence microscopy

Cells were fixed in 4% (wt/vol) paraformaldehyde for 20 minutes, washed with PBS and permeabilised with PBS containing 0.5% (vol/vol) Triton X-100 for 3 minutes. Cells were then washed with PBS, incubated with primary antibodies for 45 minutes at room temperature, washed with PBS and incubated for a further 45 minutes with the appropriate secondary antibodies at room temperature. After washing, coverslips were mounted using Prolong Gold mounting medium (Invitrogen), dried overnight at room temperature in the dark and stored at 4℃ prior to analysis.

Unless stated otherwise, all images were acquired on a DeltaVision RT restoration microscope (Applied Precision) using a 60×/NA 1.42 Plan Apo objective and the Sedat Quad Set filter set (Chroma 86000v2). The images were collected using a Coolsnap HQ camera (Photometrics) and analysed with ImageJ software. Image co-localisation analysis was performed using the Intensity Correlation Analysis ImageJ plug-in to create PDM (product of the differences from the mean) images, where PDM = (red intensity−mean red intensity)×(green intensity−mean green intensity).

Proximity ligation assay

Proximity ligation assays were performed according to the manufacturer's instructions (Duolink) using the Duolink *In Situ* PLA Probes Anti-Rabbit PLUS and Anti-Mouse MINUS, and the Duolink *In Situ* Detection Reagents Red (Sigma). Cells were counterstained using FITC–phalloidin (Invitrogen), imaged using a DeltaVision RT restoration microscope, and analysed using ImageJ. The number of positive PLA spots was quantified, for each cell, using the particle analysis plugin of ImageJ.

Live-cell fluorescence microscopy

For optimal image resolution, normal culture medium was replaced by Ham's F-12 (Gibco) containing 25 mM HEPES in the absence (Rac1 activity measurement by FLIM) or presence (membrane protrusion analyses) of 2% (vol/vol) FCS, prior to image acquisition. For analyses of membrane protrusion, U2OS cells transiently expressing Lifeact-mEGFP were plated on FN on four-compartment glass-bottom dishes (Greiner Bio-One) for 4 hours and then imaged at 37℃ on an Axiovert 200M live cell imaging system (Carl Zeiss) using a 63×/NA 1.40 Plan Apochromat objective, the 62HE filter set and a 470 nm Colibri light-emitting diode fluorescent light source (Carl Zeiss). Images were collected with a Coolsnap HQ camera using μManager (version 1.4) (Edelstein et al., 2010) at 3 minute intervals for 7 hours. The outline of each cell was segmented, divided into 400 points connected by edges, and these 400 points were tracked over the recording period using the ImageJ plug-in, QuimP11 (Tyson et al., 2010). The instant velocity of each of the 400 points was calculated between each frame using QuimP11 and velocity maps of the cell outline were generated using the QuimP11 MATLAB script in MATLAB (MathWorks). The average membrane velocity was calculated for each cell as an average of the absolute values of the instant velocity of the 400 points over the recording period.

For analysis of Rac1 activity by FLIM, U2OS and 3T3 cells transiently expressing the Raichu-Rac1 probe (Raichu-1011X) (Itoh et al., 2002), were plated on FN on four-compartment glass-bottom dishes (Greiner Bio-One) for 30 minutes and then imaged at 37℃. Images were collected using a frequency domain FLIM system (Marianis system) equipped with Lambert instruments FLIM module (3i) and a 100× objective at 15 minute intervals for 1 hour. Image analysis was performed using Slidebook (3i) and the polar plot method to calculate nearest single lifetime of CFP. Förster resonance energy transfer (FRET) efficiency was calculated using the following formula: FRET efficiency (%) = $100*(1-t_{da}/t_d)$ where 't_d' represents the lifetime of the donor (CFP; experimentally derived as 2.4594587 nseconds), and 't_{da}' represents the lifetime of the donor in the presence of the acceptor (CFP/YFP probe).

Cell migration on CDM

To generate CDM, HFFs were seeded at a density of 50,000 cells/ml in a 24-well plate. When confluent, cells were cultured for a further 10 days, with medium changed every 48 hours to complete medium supplemented with 50 μg/ml ascorbic acid (Sigma-Aldrich) to ensure collagen cross-linking. Mature matrices were then denuded of cells using lysis buffer (PBS containing 20 mM NH_4OH and 0.5% (vol/vol) Triton X-100). Following PBS washes, matrices were incubated with 10 μg/ml DNase I (Roche) at 37℃ for 30 minutes. Matrices were then stored in PBS containing 1% (vol/vol) penicillin/streptomycin and 1% (vol/vol) Fungizone at 4℃ prior to use.

For cell migration analyses, MEFs and U2OS cells were seeded at a density of 5,000 cells/ml on CDM and allowed to spread for 4 hours. Cells were then filmed using an AS MDW live-cell imaging system (Leica) with a 5×/NA 0.15 HC Plan Fluotar air objective (magnification, 1.5×). Point visiting was used to allow multiple positions to be imaged within the same time course, and cells were maintained at 37℃ and 5% (vol/vol) CO_2. Images were collected using a Coolsnap HQ camera, and eight movies (one picture every 10 minutes) were generated for each condition. To assess cell migration, the speed and directionality of 80 cells was measured (10 cells per movie) using the Manual Tracking plug-in of ImageJ. Cell tracking was performed over a 16 hour time period. Results were computed and analysed by the ImageJ plug-in Chemotaxis Tool.

Mass spectrometric data acquisition and analysis

Protein samples were separated by SDS-PAGE and allowed to migrate 10 mm into a 4–12% polyacrylamide gel. Following staining with InstantBlue (Expedeon), gel lanes were sliced into five 2-mm bands and subjected to in-gel digestion with trypsin as described previously (Shevchenko et al., 1996) with modifications (Humphries et al., 2009).

Samples were analysed by liquid chromatography tandem mass spectrometry using a nanoACQUITY UltraPerformance liquid chromatography system (Waters) coupled online to an LTQ Velos (Thermo Fisher Scientific). Peptides were concentrated and desalted on a Symmetry C18 pre-column (20 mm×180 μm, 5 μm particle size; Waters) and separated on a bridged ethyl hybrid C18 analytical column (250 mm×75 μm, 1.7 μm particle size; Waters) using a 45-minute linear gradient from 1% to 25% (vol/vol) acetonitrile in 0.1% (vol/vol) formic acid at a flow rate of 200 nl/minute. Peptides were selected for fragmentation automatically by data-dependent analysis.

Tandem mass spectra were extracted using extract_msn (Thermo Fisher Scientific) executed in Mascot Daemon (version 2.2.2; Matrix Science). Peak list files were searched against the IPI Human database (version 3.70, March 2010) modified to contain ten additional contaminant and reagent sequences of non-human origin. Searches were submitted to an in-house Mascot server (version 2.2.03; Matrix Science) (Perkins et al., 1999). Carbamidomethylation of cysteine was set as a fixed modification and oxidation of methionine was allowed as a variable modification. Only tryptic peptides were considered, with up to one missed cleavage permitted. Monoisotopic precursor mass values were used, and only doubly and triply charged precursor ions were considered. Mass tolerances for precursor and fragment ions were 0.4 Da and 0.5 Da, respectively. Data were further analysed using the search engine X! Tandem (version 2007.01.01.1) (Craig and Beavis, 2003) implemented from within Scaffold (version 3.00.03; Proteome Software). Data were validated in Scaffold using a threshold of identification of at least 90% probability at the peptide level, at least 99% probability at the protein level and assignment of at least two unique, validated peptides. These acceptance criteria resulted in an estimated protein false discovery rate of 0.1% for all datasets.

Three biological replicates were performed for each GFP pull-down. Relative protein abundance was calculated using the unweighted spectral count of a given protein normalised to the total number of spectra observed in the entire sample and to the molecular weight of that protein (normalised spectral count). Proteins in the FLNa–GFP and IQGAP1–GFP datasets enriched more than twofold over controls (GFP and RCC2) were considered to be specifically recruited. For the Rac1–GFP dataset, since RCC2 has been previously reported to interact with Rac1 (Mollinari et al., 2003), GFP was used as the negative control. Data were converted using PRIDE Converter (version 2.5.5) (Barsnes et al., 2009) and deposited in the PRIDE database (http://www.ebi.ac.uk/pride) (Vizcaíno et al., 2010) under accession numbers 26836–26850. Details of all identified proteins are provided in supplementary material Tables S1–S4.

Gene Ontology analysis was performed using DAVID (version 6.7) (Huang et al., 2009). Proteins annotated with the Gene Ontology term 'GTPase regulator activity' (GO:0030695) were selected as GTPase regulators. Proteins were hierarchically clustered on the basis of uncentred Pearson correlation using Cluster 3.0 (C Clustering Library, version 1.50) (de Hoon et al., 2004) and visualised using Java TreeView (version 1.1.6r2) (Saldanha, 2004). PPI network analysis was performed using Cytoscape (version 2.8.1) (Smoot et al., 2011). Proteins were mapped onto a merged human interactome consisting of PPIs reported in the Protein Interaction Network Analysis platform Homo sapiens network (June 2011) (Wu et al., 2009) and literature-curated databases of integrin adhesion-associated proteins (Zaidel-Bar et al., 2007), FLNa and IQGAP1 binders and Rac1 regulators (this study).

Statistical analysis

Statistical analysis was performed when appropriate, and *P* values are indicated by an asterisk in the figure legends. *Z*-tests were performed when the sample size was higher than 30, in all other cases the Student's *t*-test was used (unpaired, two-tailed, unequal variance).

Acknowledgements

We thank Fumihiko Nakamura (Brigham and Women's Hospital, Boston, MA), Kozo Kaibuchi (Nagoya University School of Medicine, Nagoya, Japan), Roland Wedlich-Söldner (Max Planck Institute of Biochemistry, Martinsried, Germany) and Robert Grosse (Institute of Pharmacology, University of Marburg, Marburg, Germany) for providing constructs and John Wilkins (University of Manitoba, Winnipeg, MB, Canada) for the JB1A antibody. We thank Alexandre Carisey (University of Manchester, Manchester, UK) for help with the microscopy analyses. We thank Stacey Warwood and David Knight (University of Manchester) for help with the mass spectrometric analyses and Julian Selley (University of Manchester) for bioinformatic support.

Author contributtions

G.J. performed most of the experiments and wrote the manuscript. M.R.M. collected the data for the cell migration and protrusion analysis experiments. A.B. and J.D.H. assisted with the MS analysis. C.K.C. and C.S.C. provided the antibody-coated patches. P.T.C. assisted with the RacGAP1 experiments. M.J.H. supervised the entire project. M.R.M., A.B., P.T.C. and M.J.H. assisted with the redaction of the manuscript.

Funding

This work was supported by the Wellcome Trust [grant number 092015 to M.J.H.]; G.J. was supported by a Wellcome Trust PhD studentship. Deposited in PMC for release after 6 months.

Supplementary material available online at
http://jcs.biologists.org/lookup/suppl/doi:10.1242/jcs.121988/-/DC1

References

Askari, J. A., Buckley, P. A., Mould, A. P. and Humphries, M. J. (2009). Linking integrin conformation to function. *J. Cell Sci.* **122**, 165-170.

Askari, J. A., Tynan, C. J., Webb, S. E. D., Martin-Fernandez, M. L., Ballestrem, C. and Humphries, M. J. (2010). Focal adhesions are sites of integrin extension. *J. Cell Biol.* **188**, 891-903.

Awasthi, A., Samarakoon, A., Chu, H., Kamalakannan, R., Quilliam, L. A., Chrzanowska-Wodnicka, M., White, G. C., 2nd and Malarkannan, S. (2010). Rap1b facilitates NK cell functions via IQGAP1-mediated signalosomes. *J. Exp. Med.* **207**, 1923-1938.

Baldassarre, M., Razinia, Z., Burande, C. F., Lamsoul, I., Lutz, P. G. and Calderwood, D. A. (2009). Filamins regulate cell spreading and initiation of cell migration. *PLoS ONE* **4**, e7830.

Barsnes, H., Vizcaíno, J. A., Eidhammer, I. and Martens, L. (2009). PRIDE Converter: making proteomics data-sharing easy. *Nat. Biotechnol.* **27**, 598-599.

Bashour, A. M., Fullerton, A. T., Hart, M. J. and Bloom, G. S. (1997). IQGAP1, a Rac- and Cdc42-binding protein, directly binds and cross-links microfilaments. *J. Cell Biol.* **137**, 1555-1566.

Bass, M. D., Roach, K. A., Morgan, M. R., Mostafavi-Pour, Z., Schoen, T., Muramatsu, T., Mayer, U., Ballestrem, C., Spatz, J. P. and Humphries, M. J. (2007). Syndecan-4-dependent Rac1 regulation determines directional migration in response to the extracellular matrix. *J. Cell Biol.* **177**, 527-538.

Bastos, R. N., Penate, X., Bates, M., Hammond, D. and Barr, F. A. (2012). CYK4 inhibits Rac1-dependent PAK1 and ARHGEF7 effector pathways during cytokinesis. *J. Cell Biol.* **198**, 865-880.

Brown, M. D. and Sacks, D. B. (2006). IQGAP1 in cellular signaling: bridging the GAP. *Trends Cell Biol.* **16**, 242-249.

Byron, A., Humphries, J. D., Askari, J. A., Craig, S. E., Mould, A. P. and Humphries, M. J. (2009). Anti-integrin monoclonal antibodies. *J. Cell Sci.* **122**, 4009-4011.

Calderwood, D. A., Huttenlocher, A., Kiosses, W. B., Rose, D. M., Woodside, D. G., Schwartz, M. A. and Ginsberg, M. H. (2001). Increased filamin binding to beta-integrin cytoplasmic domains inhibits cell migration. *Nat. Cell Biol.* **3**, 1060-1068.

Canman, J. C., Lewellyn, L., Laband, K., Smerdon, S. J., Desai, A., Bowerman, B. and Oegema, K. (2008). Inhibition of Rac by the GAP activity of centralspindlin is essential for cytokinesis. *Science* **322**, 1543-1546.

Casteel, D. E., Turner, S., Schwappacher, R., Rangaswami, H., Su-Yuo, J., Zhuang, S., Boss, G. R. and Pilz, R. B. (2012). Rho isoform-specific interaction with IQGAP1 promotes breast cancer cell proliferation and migration. *J. Biol. Chem.* **287**, 38367-38378.

Chuang, T. H., Bohl, B. P. and Bokoch, G. M. (1993). Biologically active lipids are regulators of Rac.GDI complexation. *J. Biol. Chem.* **268**, 26206-26211.

Craig, R. and Beavis, R. C. (2003). A method for reducing the time required to match protein sequences with tandem mass spectra. *Rapid. Commun. Mass. Spectrom.* **17**, 2310-2316.

David, S., Ghosh, C. C., Mukherjee, A. and Parikh, S. M. (2011). Angiopoietin-1 requires IQ domain GTPase-activating protein 1 to activate Rac1 and promote endothelial barrier defense. *Arterioscler. Thromb. Vasc. Biol.* **31**, 2643-2652.

de Hoon, M. J. L., Imoto, S., Nolan, J. and Miyano, S. (2004). Open source clustering software. *Bioinformatics* **20**, 1453-1454.

Del Pozo, M. A. and Schwartz, M. A. (2007). Rac, membrane heterogeneity, caveolin and regulation of growth by integrins. *Trends Cell Biol.* **17**, 246-250.

Edelstein, A., Amodaj, N., Hoover, K., Vale, R. and Stuurman, N. (2010). Computer control of microscopes using μManager. *Current protocols in molecular biology* **Chapter 14**, Unit14.20.

Ehrlicher, A. J., Nakamura, F., Hartwig, J. H., Weitz, D. A. and Stossel, T. P. (2011). Mechanical strain in actin networks regulates FilGAP and integrin binding to filamin A. *Nature* **478**, 260-263.

Eng, K., Naqvi, N. I., Wong, K. C. and Balasubramanian, M. K. (1998). Rng2p, a protein required for cytokinesis in fission yeast, is a component of the actomyosin ring and the spindle pole body. *Curr. Biol.* **8**, 611-621.

Estey, M. P., Di Ciano-Oliveira, C., Froese, C. D., Bejide, M. T. and Trimble, W. S. (2010). Distinct roles of septins in cytokinesis: SEPT9 mediates midbody abscission. *J. Cell Biol.* **191**, 741-749.

Galbraith, C. G., Yamada, K. M. and Galbraith, J. A. (2007). Polymerizing actin fibers position integrins primed to probe for adhesion sites. *Science* **315**, 992-995.

Gay, O., Gilquin, B., Nakamura, F., Jenkins, Z. A. and Mccartney, R. (2011). RefilinB (FAM101B) targets FilaminA to organize perinuclear actin networks and regulates nuclear shape. *PNAS*

Griffiths, G. S., Grundl, M., Allen, J. S., 3rd and Matter, M. L. (2011). R-Ras interacts with filamin a to maintain endothelial barrier function. *J. Cell. Physiol.* **226**, 2287-2296.

Guilluy, C., Garcia-Mata, R. and Burridge, K. (2011). Rho protein crosstalk: another social network? *Trends Cell Biol.* **21**, 718-726.

Hart, M. J., Callow, M. G., Souza, B. and Polakis, P. (1996). IQGAP1, a calmodulin-binding protein with a rasGAP-related domain, is a potential effector for cdc42Hs. *EMBO J.* **15**, 2997-3005.

Hauf, S., Waizenegger, I. C. and Peters, J. M. (2001). Cohesin cleavage by separase required for anaphase and cytokinesis in human cells. *Science* **293**, 1320-1323.

Hirose, K., Kawashima, T., Iwamoto, I., Nosaka, T. and Kitamura, T. (2001). MgcRacGAP is involved in cytokinesis through associating with mitotic spindle and midbody. *J. Biol. Chem.* **276**, 5821-5828.

Ho, Y.-D., Joyal, J. L., Li, Z. and Sacks, D. B. (1999). IQGAP1 integrates Ca2+/calmodulin and Cdc42 signaling. *J. Biol. Chem.* **274**, 464-470.

Hu, B., Shi, B., Jarzynka, M. J., Yiin, J. J. J., D'Souza-Schorey, C. and Cheng, S.-Y. Y. (2009). ADP-ribosylation factor 6 regulates glioma cell invasion through the IQ-domain GTPase-activating protein 1-Rac1-mediated pathway. *Cancer Res.* **69**, 794-801.

Huang, W., Sherman, B. T. and Lempicki, R. A. (2009). Systematic and integrative analysis of large gene lists using DAVID bioinformatics resources. *Nat. Protoc.* **4**, 44-57.

Humphries, J. D., Byron, A., Bass, M. D., Craig, S. E., Pinney, J. W., Knight, D. and Humphries, M. J. (2009). Proteomic analysis of integrin-associated complexes identifies RCC2 as a dual regulator of Rac1 and Arf6. *Sci. Signal.* **2**, ra51.

Hynes, R. O. (2002). Integrins: bidirectional, allosteric signaling machines. *Cell* **110**, 673-687.

Itoh, R. E., Kurokawa, K., Ohba, Y., Yoshizaki, H., Mochizuki, N. and Matsuda, M. (2002). Activation of Rac and Cdc42 video-imaged by FRET-based singlemolecule probes in the membrane of living cells. *Mol. Cell. Biol.* **22**, 6582-6591.

Jeong, H.-W., Li, Z., Brown, M. D. and Sacks, D. B. (2007). IQGAP1 binds Rap1 and modulates its activity. *J. Biol. Chem.* **282**, 20752-20762.

Katoh, H. and Negishi, M. (2003). RhoG activates Rac1 by direct interaction with the Dock180-binding protein Elmo. *Nature* **424**, 461-464.

Kiema, T., Lad, Y., Jiang, P., Oxley, C. L., Baldassarre, M., Wegener, K. L., Campbell, I. D., Ylänne, J. and Calderwood, D. A. (2006). The molecular basis of filamin binding to integrins and competition with talin. *Mol. Cell* **21**, 337-347.

Krishnan, S., Fernandez, G. E., Sacks, D. B. and Prasadarao, N. V. (2012). IQGAP1 mediates the disruption of adherens junctions to promote Escherichia coli K1 invasion of brain endothelial cells. *Cell. Microbiol.* **14**, 1415-1433.

Kuo, J. C., Han, X., Hsiao, C.-T., Yates, J. R., 3rd and Waterman, C. M. (2011). Analysis of the myosin-II-responsive focal adhesion proteome reveals a role for β-Pix in negative regulation of focal adhesion maturation. *Nat. Cell Biol.* **13**, 383-393.

Kuroda, S., Fukata, M., Kobayashi, K., Nakafuku, M., Nomura, N., Iwamatsu, A. and Kaibuchi, K. (1996). Identification of IQGAP as a putative target for the small GTPases, Cdc42 and Rac1. *J. Biol. Chem.* **271**, 23363-23367.

Lee, K. S., Yuan, Y. L., Kuriyama, R. and Erikson, R. L. (1995). Plk is an M-phase-specific protein kinase and interacts with a kinesin-like protein, CHO1/MKLP-1. *Mol. Cell. Biol.* **15**, 7143-7151.

Lehtonen, S., Ryan, J. J., Kudlicka, K., Iino, N., Zhou, H. and Farquhar, M. G. (2005). Cell junction-associated proteins IQGAP1, MAGI-2, CASK, spectrins, and alpha-actinin are components of the nephrin multiprotein complex. *Proc. Natl. Acad. Sci. USA* **102**, 9814-9819.

Leung, R., Wang, Y., Cuddy, K., Sun, C., Magalhaes, J., Grynpas, M. and Glogauer, M. (2010). Filamin A regulates monocyte migration through Rho small GTPases during osteoclastogenesis. *J. Bone Miner. Res.* **25**, 1077-1091.

Liu, S., Kapoor, M. and Leask, A. (2009). Rac1 expression by fibroblasts is required for tissue repair in vivo. *Am. J. Pathol.* **174**, 1847-1856.

Machacek, M., Hodgson, L., Welch, C., Elliott, H., Pertz, O., Nalbant, P., Abell, A., Johnson, G. L., Hahn, K. M. and Danuser, G. (2009). Coordination of Rho GTPase activities during cell protrusion. *Nature* **461**, 99-103.

Minoshima, Y., Kawashima, T., Hirose, K., Tonozuka, Y., Kawajiri, A., Bao, Y. C., Deng, X., Tatsuka, M., Narumiya, S., May, W. S., Jr et al. (2003). Phosphorylation by aurora B converts MgcRacGAP to a RhoGAP during cytokinesis. *Dev. Cell* **4**, 549-560.

Mollinari, C., Reynaud, C., Martineau-Thuillier, S., Monier, S., Kieffer, S., Garin, J., Andreassen, P. R., Boulet, A., Goud, B., Kleman, J. P. et al. (2003). The mammalian passenger protein TD-60 is an RCC1 family member with an essential role in prometaphase to metaphase progression. *Dev. Cell* **5**, 295-307.

Mondal, G., Rowley, M., Guidugli, L., Wu, J., Pankratz, V. S. and Couch, F. J. (2012). BRCA2 localization to the midbody by filamin A regulates cep55 signaling and completion of cytokinesis. *Dev. Cell* **23**, 137-152.

Morgan, M. R., Humphries, M. J. and Bass, M. D. (2007). Synergistic control of cell adhesion by integrins and syndecans. *Nat. Rev. Mol. Cell Biol.* **8**, 957-969.

Mould, A. P., Garratt, A. N., Askari, J. A., Akiyama, S. K. and Humphries, M. J. (1995). Identification of a novel anti-integrin monoclonal antibody that recognises a ligand-induced binding site epitope on the beta 1 subunit. *FEBS Lett.* **363**, 118-122.

Mould, A. P., Akiyama, S. K. and Humphries, M. J. (1996). The inhibitory anti-beta1 integrin monoclonal antibody 13 recognizes an epitope that is attenuated by ligand occupancy. Evidence for allosteric inhibition of integrin function. *J. Biol. Chem.* **271**, 20365-20374.

Nakajima, E., Suzuki, K. and Takahashi, K. (2005). Mitotic dissociation of IQGAP1 from Rac-bound beta1-integrin is mediated by protein phosphatase 2A. *Biochem. Biophys. Res. Commun.* **326**, 249-253.

Nieves, B., Jones, C. W., Ward, R., Ohta, Y., Reverte, C. G. and LaFlamme, S. E. (2010). The NPIY motif in the integrin beta1 tail dictates the requirement for talin-1 in outside-in signaling. *J. Cell Sci.* **123**, 1216-1226.

Nishiya, N., Kiosses, W. B., Han, J. and Ginsberg, M. H. (2005). An alpha4 integrin-paxillin-Arf-GAP complex restricts Rac activation to the leading edge of migrating cells. *Nat. Cell Biol.* **7**, 343-352.

Noritake, J., Fukata, M., Sato, K., Nakagawa, M., Watanabe, T., Izumi, N., Wang, S., Fukata, Y. and Kaibuchi, K. (2004). Positive role of IQGAP1, an effector of Rac1, in actin-meshwork formation at sites of cell-cell contact. *Mol. Biol. Cell* **15**, 1065-1076.

Oceguera-Yanez, F., Kimura, K., Yasuda, S., Higashida, C., Kitamura, T., Hiraoka, Y., Haraguchi, T. and Narumiya, S. (2005). Ect2 and MgcRacGAP regulate the activation and function of Cdc42 in mitosis. *J. Cell Biol.* **168**, 221-232.

Ohta, Y., Suzuki, N., Nakamura, S., Hartwig, J. H. and Stossel, T. P. (1999). The small GTPase RalA targets filamin to induce filopodia. *Proc. Natl. Acad. Sci. USA* **96**, 2122-2128.

Ohta, Y., Hartwig, J. H. and Stossel, T. P. (2006). FilGAP, a Rho- and ROCK-regulated GAP for Rac binds filamin A to control actin remodelling. *Nat. Cell Biol.* **8**, 803-814.

Padmanabhan, A., Bakka, K., Sevugan, M., Naqvi, N. I., D'souza, V., Tang, X., Mishra, M. and Balasubramanian, M. K. (2011). IQGAP-related Rng2p organizes cortical nodes and ensures position of cell division in fission yeast. *Curr. Biol.* **21**, 467-472.

Pankov, R., Endo, Y., Even-Ram, S., Araki, M., Clark, K., Cukierman, E., Matsumoto, K. and Yamada, K. M. (2005). A Rac switch regulates random versus directionally persistent cell migration. *J. Cell Biol.* **170**, 793-802.

Pelikan-Conchaudron, A., Le Clainche, C., Didry, D. and Carlier, M. F. (2011). The IQGAP1 protein is a calmodulin-regulated barbed end capper of actin filaments: possible implications in its function in cell migration. *J. Biol. Chem.* **286**, 35119-35128.

Perkins, D. N., Pappin, D. J., Creasy, D. M. and Cottrell, J. S. (1999). Probability-based protein identification by searching sequence databases using mass spectrometry data. *Electrophoresis* **20**, 3551-3567.

Petrie, R. J., Doyle, A. D. and Yamada, K. M. (2009). Random versus directionally persistent cell migration. *Nat. Rev. Mol. Cell Biol.* **10**, 538-549.

Price, L. S., Leng, J., Schwartz, M. A. and Bokoch, G. M. (1998). Activation of Rac and Cdc42 by integrins mediates cell spreading. *Mol. Biol. Cell* **9**, 1863-1871.

Ratheesh, A., Gomez, G. A., Priya, R., Verma, S., Kovacs, E. M., Jiang, K., Brown, N. H., Akhmanova, A., Stehbens, S. J. and Yap, A. S. (2012). Centralspindlin and α-catenin regulate Rho signalling at the epithelial zonula adherens. *Nat. Cell Biol.* **14**, 818-828.

Ridley, A. J. (2006). Rho GTPases and actin dynamics in membrane protrusions and vesicle trafficking. *Trends Cell Biol.* **16**, 522-529.

Ridley, A. J., Schwartz, M. A., Burridge, K., Firtel, R. A., Ginsberg, M. H., Borisy, G., Parsons, J. T. and Horwitz, A. R. (2003). Cell migration: integrating signals from front to back. *Science* **302**, 1704-1709.

Sakurai-Yageta, M., Recchi, C., Le Dez, G., Sibarita, J.-B., Daviet, L., Camonis, J., D'Souza-Schorey, C. and Chavrier, P. (2008). The interaction of IQGAP1 with the exocyst complex is required for tumor cell invasion downstream of Cdc42 and RhoA. *J. Cell Biol.* **181**, 985-998.

Saldanha, A. J. (2004). Java Treeview—extensible visualization of microarray data. *Bioinformatics* **20**, 3246-3248.

Schiller, H. B., Friedel, C. C., Boulegue, C. and Fässler, R. (2011). Quantitative proteomics of the integrin adhesome show a myosin II-dependent recruitment of LIM domain proteins. *EMBO Rep.* **12**, 259-266.

Shevchenko, A., Wilm, M., Vorm, O., Jensen, O. N., Podtelejnikov, A. V., Neubauer, G., Shevchenko, A., Mortensen, P. and Mann, M. (1996). A strategy for identifying gel-separated proteins in sequence databases by MS alone. *Biochem. Soc. Trans.* **24**, 893-896.

Smoot, M. E., Ono, K., Ruscheinski, J., Wang, P.-L. and Ideker, T. (2011). Cytoscape 2.8: new features for data integration and network visualization. *Bioinformatics* **27**, 431-432.

Tadokoro, S., Shattil, S. J., Eto, K., Tai, V., Liddington, R. C., de Pereda, J. M., Ginsberg, M. H. and Calderwood, D. A. (2003). Talin binding to integrin beta tails: a final common step in integrin activation. *Science* **302**, 103-106.

Takahashi, K. and Suzuki, K. (2006). Regulation of protein phosphatase 2A-mediated recruitment of IQGAP1 to beta1 integrin by EGF through activation of Ca2+/calmodulin-dependent protein kinase II. *J. Cell. Physiol.* **208**, 213-219.

Tan, J. L., Liu, W., Nelson, C. M., Raghavan, S. and Chen, C. S. (2004). Simple approach to micropattern cells on common culture substrates by tuning substrate wettability. *Tissue Eng.* **10**, 865-872.

Touré, A., Dorseuil, O., Morin, L., Timmons, P., Jégou, B., Reibel, L. and Gacon, G. (1998). MgcRacGAP, a new human GTPase-activating protein for Rac and Cdc42 similar to Drosophila rotundRacGAP gene product, is expressed in male germ cells. *J. Biol. Chem.* **273**, 6019-6023.

Travis, M. A., van der Flier, A., Kammerer, R. A., Mould, A. P., Sonnenberg, A. and Humphries, M. J. (2004). Interaction of filamin A with the integrin beta 7 cytoplasmic domain: role of alternative splicing and phosphorylation. *FEBS Lett.* **569**, 185-190.

Tscharntke, M., Pofahl, R., Chrostek-Grashoff, A., Smyth, N., Niessen, C., Niemann, C., Hartwig, B., Herzog, V., Klein, H. W., Krieg, T. et al. (2007). Impaired epidermal wound healing in vivo upon inhibition or deletion of Rac1. *J. Cell Sci.* **120**, 1480-1490.

Tyson, R. A., Epstein, D. B. A., Anderson, K. I. and Bretschneider, T. (2010). High resolution tracking of cell membrane dynamics in moving cells: an electrifying approach. *Math. Model. Nat. Phenom.* **5**, 34-55.

Vizcaíno, J. A., Côté, R., Reisinger, F., Barsnes, H., Foster, J. M., Rameseder, J., Hermjakob, H. and Martens, L. (2010). The Proteomics Identifications database: 2010 update. *Nucleic Acids Res.* **38 Database issue**, D736-D742.

Wu, Y. I., Frey, D., Lungu, O. I., Jaehrig, A., Schlichting, I., Kuhlman, B. and Hahn, K. M. (2009a). A genetically encoded photoactivatable Rac controls the motility of living cells. *Nature* **461**, 104-108.

Wu, J., Vallenius, T., Ovaska, K., Westermarck, J., Mäkelä, T. P. and Hautaniemi, S. (2009b). Integrated network analysis platform for protein-protein interactions. *Nat. Methods* **6**, 75-77.

Yu, Y. Y., Dai, G., Pan, F. Y., Chen, J. and Li, C. J. (2005). Calmodulin regulates the post-anaphase reposition of centrioles during cytokinesis. *Cell Res.* **15**, 548-552.

Zaidel-Bar, R., Itzkovitz, S., Ma'ayan, A., Iyengar, R. and Geiger, B. (2007). Functional atlas of the integrin adhesome. *Nat. Cell Biol.* **9**, 858-867.

Zhao, W. M. and Fang, G. (2005). MgcRacGAP controls the assembly of the contractile ring and the initiation of cytokinesis. *Proc. Natl. Acad. Sci. USA* **102**, 13158-13163.

Movie 1. Protrusion dynamics in siCTRL U2OS cell, related to figure 6. siCTRL U2OS cells transiently expressing Lifeact-mEGFP were plated on FN for 4 h and imaged at 37°C on an Axiovert 200M live cell imaging system (Carl Zeiss) for 420 min at 1 frame every 180 s.

Movie 2. Protrusion dynamics in siFLNa U2OS cell, related to figure 6. siFLNa U2OS cells transiently expressing Lifeact-mEGFP were plated on FN for 4 h and imaged at 37°C on an Axiovert 200M live cell imaging system (Carl Zeiss) for 420 min at 1 frame every 180 s.

Movie 3. Protrusion dynamics in siIQGAP1 U2OS cell, related to figure 6. siIQGAP1 U2OS cells transiently expressing Lifeact-mEGFP were plated on FN for 4 h and imaged at 37°C on an Axiovert 200M live cell imaging system (Carl Zeiss) for 420 min at 1 frame every 180 s.

Movie 4. Protrusion dynamics in siRacGAP1 U2OS cell, related to figure 6. siRacGAP1 U2OS cells transiently expressing Lifeact-mEGFP were plated on FN for 4 h and imaged at 37°C on an Axiovert 200M live cell imaging system (Carl Zeiss) for 420 min at 1 frame every 180 s.

Table S1. Proteins identified in the FLNa-GFP, IQGAP1-GFP, Rac1-GFP, RCC2-GFP and GFP pull-downs, related to figure 4. Proteins recruited to FLNa-GFP, IQGAP1-GFP, Rac1-GFP, RCC2-GFP and GFP were analysed by liquid chromatography–tandem mass spectrometry. Three biological replicates were performed for each GFP pull-down. Relative protein abundance was calculated using the unweighted spectral count of a given protein normalised to the total number of spectra observed in the entire sample and to the molecular weight of that protein (normalised spectral count).

Download Table S1

Table S2. Proteins enriched in the FLNa-GFP pull-downs, related to figure 4. List of the proteins enriched to FLNa-GFP. Relative protein abundance was calculated using the unweighted spectral count of a given protein normalised to the total number of spectra observed in the entire sample and to the molecular weight of that protein (normalised spectral count). Proteins in the FLNa-GFP dataset enriched more than two-fold over controls (GFP and RCC2) were considered to be specifically recruited.

Download Table S2

Table S3. Proteins enriched in the IQGAP1-GFP pull-downs, related to figure 4. List of the proteins enriched to IQGAP1-GFP. Relative protein abundance was calculated using the unweighted spectral count of a given protein normalised to the total number of spectra observed in the entire sample and to the molecular weight of that protein (normalised spectral count). Proteins in the IQGAP1-GFP dataset enriched more than two-fold over controls (GFP and RCC2) were considered to be specifically recruited.

Download Table S3

Table S4. Proteins enriched in the Rac1-GFP pull-downs, related to figure 4. List of the proteins enriched to Rac1-GFP. Relative protein abundance was calculated using the unweighted spectral count of a given protein normalised to the total number of spectra observed in the entire sample and to the molecular weight of that protein (normalised spectral count). Proteins in the Rac1-GFP dataset enriched more than two-fold over the GFP control were considered to be specifically recruited.

Download Table S4

Table S5. Proteins enriched in the RCC2-GFP pull-downs, related to figure 4. List of the proteins enriched to RCC2-GFP. Relative protein abundance was calculated using the unweighted spectral count of a given protein normalised to the total number of spectra observed in the entire sample and to the molecular weight of that protein (normalised spectral count). Proteins in the RCC2-GFP dataset enriched more than two-fold over the GFP control were considered to be specifically recruited.

Download Table S5